ERDC TR-19-8

US Army Corps
of Engineers®
Engineer Research and
Development Center

ERDC
ENGINEER RESEARCH & DEVELOPMENT CENTER

Rapid Airfield Damage Recovery Technology Integration Experiment

Haley P. Bell, Benjamin C. Cox, Lulu Edwards, Lyan I. Garcia,
Nolan R. Hoffman, Mariely Mejías-Santiago,
and Jared L. Johnson

June 2019



Approved for public release; distribution is unlimited.

Engineer Research and
Development Center

The U.S. Army Engineer Research and Development Center (ERDC) solves the nation's toughest engineering and environmental challenges. ERDC develops innovative solutions in civil and military engineering, geospatial sciences, water resources, and environmental sciences for the Army, the Department of Defense, civilian agencies, and our nation's public good. Find out more at www.erdc.usace.army.mil.

To search for other technical reports published by ERDC, visit the ERDC online library at http://acwc.sdp.sirsi.net/client/default.

ERDC TR-19-8
June 2019

Rapid Airfield Damage Recovery Technology Integration Experiment

Haley P. Bell, Benjamin C. Cox, Lulu Edwards, Lyan I. Garcia,
Nolan R. Hoffman, and Mariely Mejías-Santiago

Geotechnical and Structures Laboratory
U.S. Army Engineer Research and Development Center
3909 Halls Ferry Road
Vicksburg, MS 39180-6199

Jared L. Johnson

Environmental Laboratory
U.S. Army Engineer Research and Development Center
3909 Halls Ferry Road
Vicksburg, MS 39180-6199

Final report

Approved for public release; distribution is unlimited.

Prepared for Headquarters, U.S. Air Force Civil Engineer Center
Tyndall Air Force Base, FL 32403-5319

Under Project Number 463347

Abstract

The traditional crater repair equipment and materials developed under the Rapid Airfield Damage Recovery (RADR) program, while highly capable, are large, expensive, and logistically challenging. Research projects from 2016 and 2017 identified lighter and leaner crater repair equipment and backfill materials in an attempt to decrease some of the economic and logistical burdens on the U.S. Air Force. The RADR Technology Integration Experiment assessed the lighter and leaner equipment, materials, and methods for small crater repairs in a relative full-scale environment. The experiment was conducted in August 2017 at the Silver Flag Exercise Site located at Tyndall Air Force Base, FL. The lighter and leaner technologies were compared with the traditional crater repair process. Flowable fill, polyurethane foam, cement-stabilized soil, and geocells with granular fill were proven to be viable backfill options for repairing craters when capped with rapid-setting concrete. This effort resulted in successful crater repair solutions using the lighter and leaner technologies with limited increases in repair time. An optimized small crater repair package was developed based on the results of this experiment.

DISCLAIMER: The contents of this report are not to be used for advertising, publication, or promotional purposes. Citation of trade names does not constitute an official endorsement or approval of the use of such commercial products. All product names and trademarks cited are the property of their respective owners. The findings of this report are not to be construed as an official Department of the Army position unless so designated by other authorized documents.

DESTROY THIS REPORT WHEN NO LONGER NEEDED. DO NOT RETURN IT TO THE ORIGINATOR.

Contents

Abstract ii

Figures and Tables v

Preface ix

Unit Conversion Factors x

1 Introduction 1

1.1 Background 1

1.2 Objective and scope 2

2 Test Site Description 3

3 Equipment and Material Descriptions 5

3.1 Traditional RADR crater repair equipment 5

3.1.1 Utility vehicles (UTVs) 5

3.1.2 Line-of-sight profile measurement devices 6

3.1.3 Compact track loaders (CTL) and attachments 6

3.1.4 Simplified volumetric concrete mixer 8

3.1.5 Telehandler 10

3.1.6 Front-end loader 10

3.1.7 Excavator with hammer and bucket attachments 11

3.1.8 Tractor truck with flatbed trailer 13

3.1.9 Water truck 14

3.1.10 Concrete finishing tools 14

3.2 Lighter and leaner RADR crater repair equipment 15

3.2.1 Mini skid steer 15

3.2.2 Diamond blade saw attachment 16

3.2.3 Backhoe loaders 17

3.2.4 Rammer 18

3.2.5 Plate compactor 19

3.2.6 Tiller attachment 19

3.2.7 Mid-size rider sweeper 21

3.2.8 FOD Boss 21

3.2.9 Telehandler screed 22

3.2.10 Deployable volumetric concrete mixer 23

3.2.11 Telehandler forklift 24

3.3 Crater repair materials 24

3.3.1 Rapid-setting flowable fill 25

3.3.2 Polyurethane foam 25

3.3.3 Silty sand 27

3.3.4 Portland limestone cement 28

3.3.5 Geocells 29

3.3.6 Rapid-setting concrete 30

4 Traditional RADR Crater Repair Process 32

5 Experiment Training Procedures and Results 40

5.1 Procedures 40
5.2 Results 41

6 Test Procedures and Results 44

6.1 Test #1: Lighter and leaner equipment; rapid-setting flowable fill backfill 45
6.1.1 Procedure 45
6.1.2 Results 51
6.2 Test #2: Lighter and leaner equipment; polyurethane foam backfill 59
6.2.1 Procedure 59
6.2.2 Results 63
6.3 Test #3: Lighter and leaner RADR equipment; cement-stabilized silty sand backfill 68
6.3.1 Procedure 68
6.3.2 Results 74
6.4 Test #4: Traditional equipment; geocells with sand backfill 80
6.4.1 Procedure 80
6.4.2 Results 85
6.5 Summary of test results 90

7 Conclusions and Recommendations 100

7.1 Conclusions 100
7.2 Recommendations 103

References 104

Report Documentation Page

Figures and Tables

Figures

Figure 2.1. Simulated bomb-damaged crater. 3
Figure 2.2. Crater repair locations. 4
Figure 3.1. UTV. 5
Figure 3.2. Marking extents of crater upheaval after using line-of-sight measurement devices. 6
Figure 3.3. Caterpillar CTLs and attachments. 7
Figure 3.4. Simplified volumetric concrete mixer – 7 yd^3. 9
Figure 3.5. Caterpillar TL1255D telehandler. 10
Figure 3.6. Caterpillar 926M front-end loader. 11
Figure 3.7. Volvo EW180C wheeled excavators with hammer and bucket attachments. 12
Figure 3.8. Tractor with flatbed trailer. 14
Figure 3.9. Water truck. 14
Figure 3.10. Wyco Screed King vibratory screed. 15
Figure 3.11. Magnesium straight-edge bar. 15
Figure 3.12. Ditch Witch SK850 mini skid steer. 16
Figure 3.13. Cuts, Inc. SS 4200 HF diamond blade saw attachment on CTL. 17
Figure 3.14. JCB 3CX (top) and 4CX (bottom) backhoe loaders. 18
Figure 3.15. Multiquip MTX-70 rammer. 19
Figure 3.16. JPC-80 vibratory plate compactor. 20
Figure 3.17. Caterpillar LT13B tiller attachment on CTL. 20
Figure 3.18. Tennant S20 mid-size rider sweeper. 21
Figure 3.19. FOD Boss 8. 22
Figure 3.20. Telehandler-powered ASTH. 22
Figure 3.21. Simplified volumetric concrete mixer – 2.5 yd^3. 23
Figure 3.22. Caterpillar TL642C telehandler. 24
Figure 3.23. Flowable fill during dry placement method. 25
Figure 3.24. Polyurethane foam during placement with dispenser in background. 26
Figure 3.25. Silty sand grain size distribution. 27
Figure 3.26. Silty sand moisture density relationship. 28
Figure 3.27. Mixing PLC with silty sand prior to placement in a crater. 29
Figure 3.28. Geocell material during measuring for cutting. 30
Figure 3.29. CTS Rapid Set Concrete Mix® during placement with the simplified volumetric mixer. 31
Figure 4.1. Completed rapid-setting concrete crater repair. 32
Figure 4.2. Debris removal with front-end loader and CTL. 33

Figure 4.3. Hauling super sacks of cementitious material. 33
Figure 4.4. Crater profile measuring using line-of-sight devices..... 34
Figure 4.5. Saw cutting around crater upheaval. 35
Figure 4.6. Breaking and excavating damaged PCC..... 35
Figure 4.7. Placing rapid-setting flowable fill backfill by using the dry method. 36
Figure 4.8. Adding water to flowable fill during dry placement method. 36
Figure 4.9. Crater repair with Rapid-Set Concrete Mix® using the volumetric mixer. 37
Figure 6.1. Typical debris field created for each test. 44
Figure 6.2. Debris removal with Ditch Witch SK850 mini track loaders. 45
Figure 6.3. Wheel saw and diamond blade saw in operation..... 46
Figure 6.4. Breaking and excavating with JCB 4CX (top) and 3CX (bottom)..... 48
Figure 6.5. Caterpillar TL642C loading small volumetric mixer. 49
Figure 6.6. Screeding crater repair with telehandler-operated ASTH..... 49
Figure 6.7. Typical final debris removal with lighter and leaner equipment. 50
Figure 6.8. HWD testing of crater repair..... 50
Figure 6.9. F-15E single-wheel load cart..... 51
Figure 6.10. Gantt chart of overall progress with lighter and leaner crater equipment and flowable fill backfill (Test #1)..... 55
Figure 6.11. Pile of dry material spilled from small volumetric mixer bin. 56
Figure 6.12. Shrinkage cracking on surface of Repair 1 (flowable fill backfill) before trafficking. 57
Figure 6.13. Low-severity joint spalling on Repair 1 (flowable fill backfill) after 3,504 passes..... 58
Figure 6.14. Prototype automated foam dispensing system with foam totes. 59
Figure 6.15. Overview of foam backfill process in Test #2..... 61
Figure 6.16. Gantt chart of overall progress with lighter and leaner crater equipment and foam backfill (Test #2). 66
Figure 6.17. Shrinkage cracks on Repair 2 with foam backfill (Test #2)..... 67
Figure 6.18. Medium-severity joint spall on foam backfill repair after 3,504 passes (Test #2). 68
Figure 6.19. Soil blending layout..... 69
Figure 6.20. Addition of water to the silty sand stockpile in Test #3..... 70
Figure 6.21. Overview of soil-blending process in Test #3. 71
Figure 6.22. Overview of cement-stabilized backfill process in Test #3. 72
Figure 6.23. Gantt chart of overall progress with lighter and leaner crater repair equipment and cement-stabilized soil backfill (Test #3)..... 78
Figure 6.24. Typical shrinkage cracking on surface of cement-stabilized soil backfill repairs (Test #3). 79
Figure 6.25. Low-severity joint spall on cement-stabilized soil backfill repair at 3,504 passes (Test #3)..... 79

Figure 6.26. Measuring and cutting geotextile fabric and geocell sections in Test #4. 82
Figure 6.27. Overview of geocell backfill installation process in Test #4. 84
Figure 6.28. Gantt chart of overall progress with traditional crater equipment and geocells with sand backfill (Test #4) 88
Figure 6.29. Medium-severity joint spalling on geocell backfill Repair 5 (Test #4). 89
Figure 6.30. Low-severity linear cracking on geocell backfill Repair 5 (Test #4). 90
Figure 6.31. Normalized average crater repair task timing summary for each test. 92
Figure 6.32. HWD data of crater repairs with various backfill material. 97

Tables

Table 3.1. Caterpillar CTL specifications. 7
Table 3.2. Wheel saw specifications 8
Table 3.3. Caterpillar TL1255D telehandler specifications 10
Table 3.4. Caterpillar 926M front-end loader specifications. 11
Table 3.5. Volvo EW180C wheeled excavator specifications. 13
Table 3.6. Volvo HB1400 excavator hammer specifications. 13
Table 3.7. Ditch Witch SK850 specifications. 16
Table 3.8. Cuts, Inc. SS 4200 HF diamond blade saw attachment specifications 17
Table 3.9. JCB 3CX and 4CX backhoe loader specifications. 18
Table 3.10. Multiquip MTX-70 rammer specifications. 19
Table 3.11. Caterpillar LT13B tiller attachment specifications. 20
Table 3.12. Tennant S30 sweeper specifications. 21
Table 3.13. Genie GTH-1256 AF specifications 23
Table 3.14. Caterpillar TL642C telehandler specifications. 24
Table 5.1. Three-crater repair training sequence timing results. 42
Table 6.1. Repair characteristics and task times for Test #1 (lighter and leaner equipment and flowable fill backfill) 52
Table 6.2. Saw-cutting rates for Test #1 53
Table 6.3. Repair characteristics and task times for Test #2 (lighter and leaner equipment and foam backfill). 63
Table 6.4. Saw-cutting rates for Test #2 65
Table 6.5. Repair characteristics and task times for Test #3 (lighter and leaner equipment and cement-stabilized silty sand backfill). 74
Table 6.6. Saw-cutting rates for Test #3 76
Table 6.7. Repair characteristics and task times for Test #4 (traditional equipment and geocell-reinforced sand backfill). 86
Table 6.8. Saw-cutting rates for Test #4 87
Table 6.9. Timing summary of lighter and leaner experiment and previous crater repair demonstrations. 91
Table 6.10. RADR experiment backfill task summary 95

Table 6.11. Cored Rapid Set Concrete Mix® thickness and compressive strength data. 96
Table 6.12. Generic RADR crater repair equipment weights and volumes for one crater repair team. 98

Preface

The Rapid Airfield Damage Recovery Integration Experiment was conducted for the U.S. Air Force Civil Engineer Center (AFCEC). The technical monitor was Dr. Robert Diltz, AFCEC.

The work was performed by the Airfields and Pavements Branch (GMA) and the Concrete and Materials Branch (GMC) of the Engineering Systems and Materials Division (GM), U.S. Army Engineer Research and Development Center (ERDC), Geotechnical and Structures Laboratory (ERDC-GSL) and the Environmental Engineering Branch (EPE) of the Environmental Processes and Engineering Division (EP), U.S. Army ERDC, Environmental Laboratory (ERDC-EL). Photography was provided by Mr. Vincent A. Mouzon, ACE-IT. Mr. Jeb S. Tingle, GM, was the RADR program manager for ERDC. At the time of publication, Dr. Timothy W. Rushing was Chief, CEERD-GMA; Dr. W. Andrew Martin was Chief, CEERD-EPE; Mr. Justin Strickler was Acting Chief, CEERD-GM; Mr. Warren P. Lorentz was Chief, CEERD-EP; and Mr. R. Nicholas Boone, CEERD-GVT, was the Technical Director for Force Projection and Maneuver Support. The Deputy Director of ERDC-GSL was Mr. Charles W. Ertle II, and the Director was Mr. Bartley P. Durst. Dr. Jack E. Davis was Deputy Director of ERDC-EL, and the Director was Dr. Ilker Adiguzel.

COL Ivan P. Beckman was the Commander of ERDC, and Dr. David W. Pittman was the Director.

Unit Conversion Factors

Multiply	By	To Obtain
cubic yards	0.7645549	cubic meters
degrees Fahrenheit	(F-32)/1.8	degrees Celsius
feet	0.3048	meters
foot-pounds force	1.355818	joules
gallons (U.S. liquid)	3.785412 E-03	cubic meters
horsepower (550 foot-pounds force per second)	745.6999	watts
inches	0.0254	meters
miles per hour	0.44704	meters per second
mils	0.0254	millimeters
pounds (force)	4.448222	newtons
pounds (force) per square inch	6.894757	kilopascals
pounds (mass)	0.45359237	kilograms
square feet	0.09290304	square meters
square inches	6.4516 E-04	square meters
tons (2,000 pounds, mass)	907.1847	kilograms
yards	0.9144	meters

1 Introduction

1.1 Background

The U.S. Air Force's Rapid Airfield Damage Recovery (RADR) Program has developed technologies and methodologies to repair bomb craters on runways and taxiways within 6.5 hr after an attack. Typically, damaged pavements must be repaired by using fast methods and durable materials to reduce the total time that the pavement is removed from service, as well as to reduce the need to conduct subsequent repairs to maintain an operable pavement surface. In addition to military wartime repairs, conventionally damaged military and civilian airfields must also be repaired quickly, and these repairs must be capable of withstanding aircraft traffic at full operational levels.

The traditional technologies used for crater repair in airfield pavements include compact track loaders (CTLs) with wheel saw, broom, and bucket attachments; wheeled excavators with bucket and pavement breaker attachments; front-end loaders; utility vehicles; extendable boom forklifts; simplified volumetric mixers; dump trucks; water trucks; flatbed trailers; rapid-setting cementitious materials; and a variety of concrete finishing tools. These technologies and the crater repair process have been tested in cold, hot and dry, and wet weather. Details and results of the previous full-scale crater repair tests can be found in Tingle et al. 2009, Priddy et al. 2013a, Priddy et al. 2013b, Pullen et al. 2014, Edwards et al. 2013, and Bell et al. 2013.

The equipment package and the materials developed under the RADR program for repairing craters, described in the previous paragraph, have been successfully assessed in many scenarios and are capable of supporting more than 3,500 passes of fully loaded military aircraft. However, the traditional crater repair equipment set and materials are large, expensive, and logistically challenging. A "lighter and leaner" equipment package and innovative repair materials are needed to decrease some of the economic and logistical burdens on the U.S. Air Force.

Separate research projects involving the various tasks of small crater repair were completed in 2016 and 2017 with the objectives of identifying and evaluating lighter and leaner equipment and backfill materials. The

various projects identified the most promising lighter and leaner material-handling equipment (Robinson et al. 2016), debris-removal equipment (Strange et al. 2017), saw-cutting equipment (Bell and Rowland 2017), excavation equipment, and a deployable volumetric mixer for rapid-setting concrete capping. Novel backfill materials including polyurethane foam, geocells with granular fill, and cement-stabilized soil were also successfully tested under rapid-setting concrete caps with simulated aircraft traffic. The most promising lighter and leaner equipment and materials identified in the separate tasks for crater repair integrated into a combined equipment package and evaluated in an all-encompassing, full-scale crater repair scenario.

1.2 Objective and scope

The primary objective of this project was to evaluate the lighter and leaner equipment, materials, and methods for small crater repairs in an encompassing and relative full-scale environment. The project also included repairs conducted using the traditional crater repair equipment and materials for comparison. The experiment described in this report gathered trade-space data for the optimization of equipment, materials, and processes used for small crater repairs.

The objectives were accomplished by training a group of 28 Airmen in crater repair techniques using the traditional RADR crater repair equipment, materials, and methods as well as the lighter and leaner crater repair equipment, materials, and methods. The Airmen were trained on backfill placement using rapid-setting flowable fill, geocells with sand fill, cement-stabilized silty sand, and polyurethane foam. Four different crater repair sequences were timed; one test used all traditional RADR equipment and three tests used the lighter and leaner equipment. Simulated F-15E aircraft traffic was applied to each of the crater repairs following the completion of each field test to validate the structural adequacy of the completed repairs.

Chapter 2 describes the test site. Chapter 3 presents the equipment and materials included in the experiment, and Chapter 4 summarizes the traditional RADR crater repair process. Chapter 5 lists the training procedures and results. Chapter 6 describes the traditional RADR and lighter and leaner RADR crater repair experiments, including the weather conditions, timeline, and results. Conclusions and recommendations are included in Chapter 7.

2 Test Site Description

The small crater repair tests using the traditional RADR equipment set and the lighter and leaner RADR equipment set took place from 23 to 31 August 2017 at the Silver Flag Exercise Site located at Tyndall Air Force Base, FL. Twenty slabs located sporadically along the south end of the training runway had been previously exploded to simulate bomb crater damage. The damaged slabs were used for the crater repair tests described in this report. Figure 2.1 shows one of the 20 simulated bomb-damaged craters.

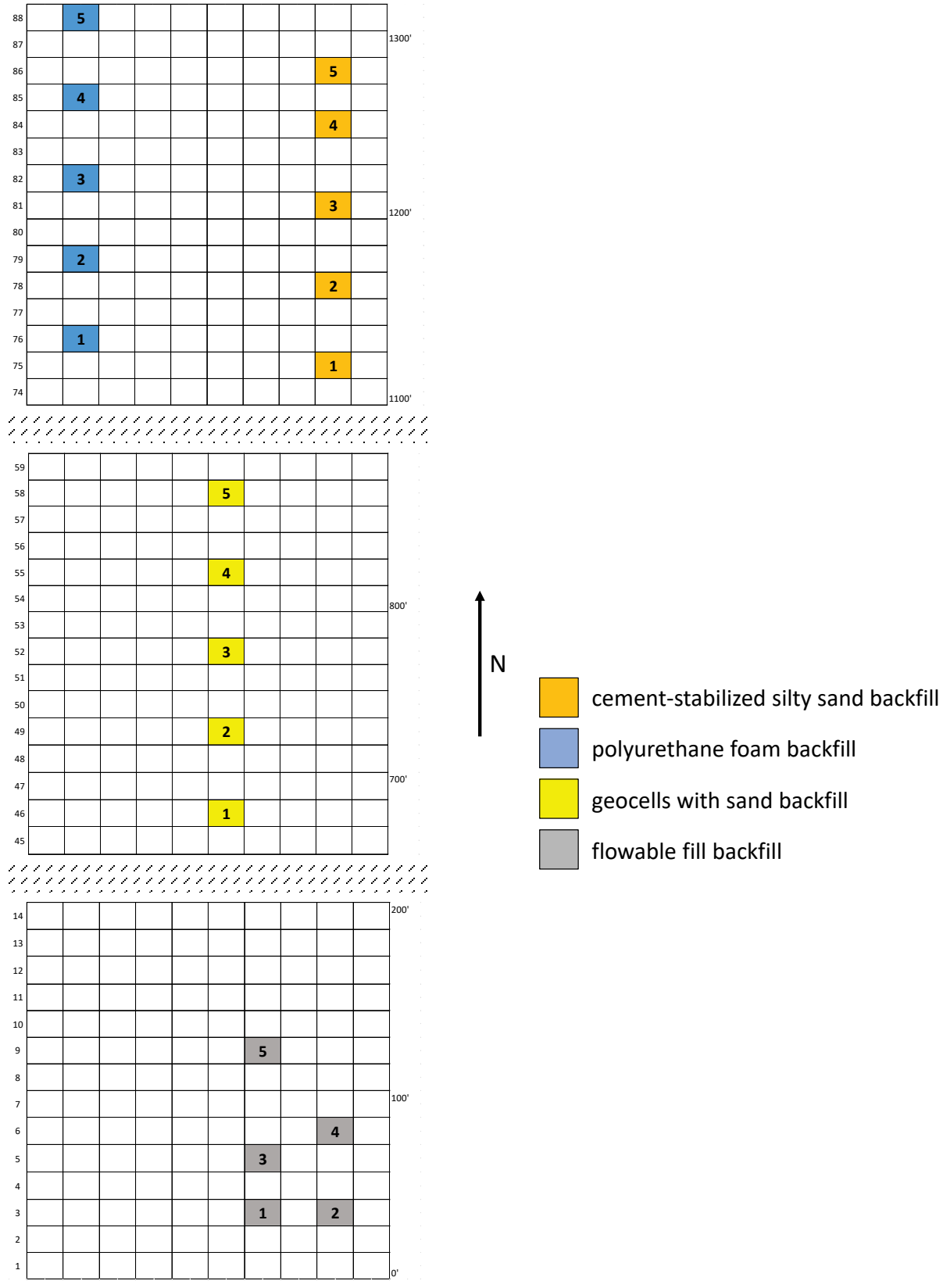
Figure 2.1. Simulated bomb-damaged crater.



Each portland cement concrete (PCC) slab was approximately 15 ft by 15 ft, and the apparent diameter of each blown crater varied from 6.5 ft to 15 ft. Small craters are typically 15 ft in diameter or less, while large craters are greater than 15 ft in diameter. The thickness of the slabs ranged from 8 in. to 18 in. The compressive strengths of the parent slabs varied from approximately 3,000 psi to 8,000 psi (Pullen et al. 2014).

Figure 2.2 shows the layout of the craters for the four tests. Five slabs were grouped for each of the four tests, each with different backfill materials. All crater repairs were capped with 10 in. of rapid-setting concrete.

Figure 2.2. Crater repair locations.



3 Equipment and Material Descriptions

Most crater repairs on the PCC pavements at the Silver Flag Exercise Site were completed by using the lighter and leaner equipment selected for the full-scale integration testing. The selected equipment showed potential in separate smaller-scale projects. The crater repairs were also completed by using three novel backfill materials -- polyurethane foam, cement-stabilized silty sand, and geocells with sand fill -- as well as flowable fill, the traditional backfill material for crater repairs in the RADR kits.

The following sections describe the traditional RADR crater repair equipment and materials and the lighter and leaner equipment and materials used to complete the crater repair tests with rapid-setting concrete caps.

3.1 Traditional RADR crater repair equipment

3.1.1 Utility vehicles (UTVs)

UTVs (Figure 3.1) were used to transport team members, tools, and equipment from the staging area to the repair site; they are not included in the official crater repair equipment set. The crater team leader used a UTV for personal transportation and to carry tape measures, shovels, rakes, brooms, paint crayons, spray paint, utility knives, and extra personal protective equipment (PPE). The marking team and backfill team also used UTVs to carry some of the personnel and the marking, backfill, and capping equipment. UTVs were also used for the lighter and leaner tests.

Figure 3.1. UTV.



3.1.2 Line-of-sight profile measurement devices

Line-of-sight profile measurement devices were used in the crater profile measurement (CPM) process to determine the extent of upheaval around each crater, as shown in Figure 3.2. The CPM process utilized two "T" stanchions, a sight rod, a straight edge, and spray paint. The line-of-sight profile measurement devices are typically used again after the repairs are completed to ensure that each repair met the repair quality criterion. More information about the stanchion construction and its use in the CPM process can be found in the Technical Order (T.O.) 35E2-5-1 (United States Air Force 1992). Line-of-sight profile measurement devices were also used for the lighter and leaner tests.

Figure 3.2. Marking extents of crater upheaval after using line-of-sight measurement devices.



3.1.3 Compact track loaders (CTL) and attachments

Caterpillar 279C XPS, 279D XPS, and 289D XPS model CTLs -- or skid steers -- are rubber-tracked machines with high-flow hydraulics employed for a variety of purposes in the RADR process (Figure 3.3). The CTLs were used for rapidly cutting around the upheaval by using wheel-saw attachments, removing debris using bucket attachments, and cleanup by using broom attachments. The machines were equipped with quick-disconnect fittings that allowed the attachments to be exchanged rapidly without the use of tools. Table 3.1 includes the specifications for the 279C XPS, 279D XPS, and 289D XPS model CTLs. The CTLs were also used for the lighter and leaner tests.

Figure 3.3. Caterpillar CTLs and attachments.



Table 3.1. Caterpillar CTL specifications.

Specification	Caterpillar 279C XPS	Caterpillar 279D XPS	Caterpillar 289D XPS
Net Power (hp)	82	72.9	72.9
Operating Weight (lb)	9,945	9,893	10,533
Rated Operating Capacity at 50% Tipping Load (lb)	3,200	2,935	3,800
Travel Speed (mph)	5.0	4.5	4.5
Tipping Load (lb)	6,483	5,870	7,600
Breakout Force (lb)	7,308	7,285	7,291
Max Loader Hydraulic Pressure (psi)	4,061	4,061	4,061
Max Loader Hydraulic Flow (gal/min)	33	32	32
Overall Length (in.)	116.4	117.9	117.9
Height – Top of Cab (in.)	82.8	83.2	83.2
Width (in.)	78.0	78.0	78.0

The Caterpillar 279C XPS CTL is no longer manufactured but was the original model tested and selected for traditional RADR crater repairs. The 279D XPS and 289D XPS models are newer versions with enhanced features. The length, width, and height dimensions of all three models are

within approximately 1 in. of each other, and the operating weights are essentially the same.

3.1.3.1 Wheel-saw attachments

The Caterpillar CTLs were capable of operating the Caterpillar SW45 and/or SW360B wheel-saw attachments (Figure 3.3). The wheel-saw attachments used for crater repairs provided a 3.5-in.-wide cut. The SW45 provides an 18-in. maximum depth cut, and the SW360B provides a 24-in. maximum depth cut. The wheel saws were equipped with a hydraulic side shift to assist in wheel positioning. Specifications for both saws are included in Table 3.2. Kennametal SC3-01P conical bits were used on the wheel saws.

Table 3.2. Wheel-saw specifications.

Specification	Caterpillar SW45	Caterpillar SW360B
Overall Width (in.)	71	73
Overall Height (in.)	57	70
Length (in.)	78	93
Weight (lb)	2,295	3,420
Wheel Width (in.)	3	3
Required Hydraulic Flow (gal/min)	24 - 42	33
Optimal Hydraulic Pressure (psi)	2,611 - 4,351	3,335
Wheel Speed at Maximum Flow (rpm)	115	74
Conical Bits per Wheel	64	70
Maximum Depth of Cut (in.)	18	24
Side-Shift Travel (in.)	26	22

3.1.3.2 Bucket and angle broom attachments

Bucket and angle broom (Caterpillar BA118C) attachments (Figure 3.3) were used with the CTLs for debris removal and cleanup before, during, and/or after each crater repair test. The buckets are approximately 78 in. wide. The broom attachment is 32 in. in diameter and 84 in. wide.

3.1.4 Simplified volumetric concrete mixer

A customized tow-behind volumetric concrete mixer with simplified controls was specifically designed by CemenTech Inc. in consultation with

the U.S. Army Engineer Research and Development Center (ERDC) for the RADR program and was used for capping the crater repairs with the rapid-setting concrete. The simplified volumetric mixer is pre-calibrated for rapid-setting cementitious repair materials to include flowable fill backfill and rigid concrete capping material.

The legacy RADR mixer (Figure 3.4) was towed with a military vehicle. The mixer consisted of a single, dry-material hopper with a capacity of approximately 7 yd^3, a conveyor belt feed system, a positive displacement water pump to meter the mix water according to fixed pump speed, two 200-gal water containers on each side of the mixer, a washout container with a pressure washer, and a replaceable mixing auger. The machine was outfitted with two retractable catwalk platforms, a bin entry platform, a replacement auger, and two super-sack piercing points. A steel grate located near the bottom of the dry-material bin prevented large pieces of material from entering the conveyor belt, thereby preventing considerable damage.

Figure 3.4. Simplified volumetric concrete mixer – 7 yd^3.



The only means of controlling the water-cement ratio was by adjusting a strike-off gate that could change the height of dry material on the conveyor belt feeding the mix auger. Allowing more dry material to enter the mix auger would have resulted in a mix with a lower water-cement ratio. The wheel for adjusting the gate height had a scale from 1 to 12: 1 allowed the least amount of material to enter the mix auger, and 12 allowed the most.

3.1.5 Telehandler

Caterpillar TL1255D telehandlers (Figure 3.5) were used for transporting and loading the volumetric concrete mixer with super sacks of the rapid-setting concrete materials. The super sacks of cementitious material weighed approximately 3,000 lb. Table 3.3 gives specifications of the Caterpillar TL1255D telehandler.

Figure 3.5. Caterpillar TL1255D telehandler.



Table 3.3. Caterpillar TL1255D telehandler specifications.

Maximum Gross Power (hp)	142.1
Operating Weight (lb)	34,361
Rated Load Capacity (lb)	12,000
Maximum Lift Height (ft)	54.6
Maximum Forward Reach (ft)	42.0
Maximum Travel Speed (mph)	20.5
Length (ft)	20.7
Width (ft)	8.3
Height (ft)	8.3

3.1.6 Front-end loader

A Caterpillar 926M front-end loader (Figure 3.6) was used for initial debris removal. The front-end loader was equipped with a 2.5-yd^3 bucket. Specifications of the front-end loader are shown in Table 3.4.

Figure 3.6. Caterpillar 926M front-end loader.



Table 3.4. Caterpillar 926M front-end loader specifications.

Maximum Gross Power (hp)	153
Maximum Gross Torque (lbf-ft)	531
Operating Weight (lb)	28,770
Maximum Travel Speed (mph)	25
Maximum Flow (gal/min)	40

3.1.7 Excavator with hammer and bucket attachments

A Volvo EW180C wheeled excavator with an HB1400 moil-tipped hammer was used to break the PCC during the testing. A separate Volvo EW180C wheeled excavator with a 24-in.-wide toothed bucket was used for excavating the broken PCC and any loose base course material. The teeth on the bucket were 7 in. long. The excavators with the hammer and bucket attachments are shown in Figure 3.7.

Figure 3.7. Volvo EW180C wheeled excavators with hammer and bucket attachments.



Wheeled excavators are preferred to tracked excavators for crater repair purposes since wheeled excavators are faster and minimize damage to the existing pavement around the repairs. The excavator was equipped with quick-disconnect fittings for exchanging the hammer and bucket work tool attachments, if needed. Specifications for the Volvo EW180C are listed in Table 3.5, and specifications for the Volvo HB1400 hammer are listed in Table 3.6.

Table 3.5. Volvo EW180C wheeled excavator specifications.

Gross Power (hp)	164
Maximum Torque (lb-ft)	538 (at 1,350 rpm)
Maximum Digging Reach (ft)	31
Maximum Digging Depth (ft)	20.4
Maximum Travel Speed (mph)	21.7
Operating Weight (lb)	42,946
Overall Width (ft)	8.3
Shipping Length (ft)	29
Height to Top of Cab (ft)	10.4

Table 3.6. Volvo HB1400 excavator hammer specifications.

Impact Energy (lb-ft)	2,500
Operating Weight (lb)	2,932
Tool Diameter (in.)	4.92
Acceptable Oil Flows (gal/min)	32 to 45
Oil Pressure (psi)	1,958 to 2,103
Impact Rate (blows per min)	450 to 800
Excavator Weight Limits (lb)	39,683 to 57,320

3.1.8 Tractor truck with flatbed trailer

A 10-ton tractor truck with a 40-ft-long flatbed trailer (Figure 3.8) was used to transport the super sacks containing flowable fill and rapid-setting concrete materials from the staging area to the repair area. The 40-ft-long flatbed trailer was capable of transporting a maximum of 14 super sacks from the dry storage area to the repair site. Material was off-loaded with extendable boom forklifts and staged near the repair sites for loading rapid-setting concrete into the volumetric mixer or flowable fill directly into the excavation. The tractor-trailer was also used for the lighter and leaner tests.

Figure 3.8. Tractor with flatbed trailer.



3.1.9 Water truck

Two commercial water trucks with a 2,000-gal capacity (Figure 3.9) were needed for the backfilling and capping processes. Water is required when placing dry flowable fill backfill and for the volumetric mixer's water tanks to mix rapid-setting concrete for the surface capping of the repairs. A 2-in.-diam hose connection was used to provide water for these activities. The water trucks were equipped with a power takeoff, or a pump powered by the vehicle drive system. The water trucks were also used for the lighter and leaner tests.

Figure 3.9. Water truck.



3.1.10 Concrete finishing tools

The repairs were struck off by using a vibratory screed consisting of a 10-ft-long magnesium screed bar with a small engine (Figure 3.10). The screed used was a Screed King manufactured by Wyco Tool, powered by a 1.25-hp Honda GX35 gasoline engine. The screed was moved across the repair with one person pulling at the motor and two people applying pressure at each end to ensure the repair was level. Minimal hand finishing was performed after screeding by using aluminum or magnesium trowels. Repairs greater than approximately 9 ft by 9 ft were struck off by hand by using a 17-ft-long magnesium straight-edge bar (Figure 3.11).

Figure 3.10. Wyco Screed King vibratory screed.



Figure 3.11. Magnesium straight-edge bar.



3.2 Lighter and leaner RADR crater repair equipment

Equipment, such as the UTVs (Section 3.1.1), the stanchions (Section 3.1.2), the CTLs with wheel-saw attachments (Sections 3.1.3 and 3.1.3.1), and the water trucks (Section 3.1.9), was also used in the lighter and leaner equipment sets. The following sections describe the additional crater repair equipment and tools that were used in the experiment as replacements for the majority of the traditional RADR equipment.

3.2.1 Mini skid steer

A Ditch Witch SK850 mini skid steer (Figure 3.12) was used for debris removal around the repair sites. The machine featured a 332 in.^{2} stand-on platform and utilized standard dual-level ground drive controls. The mini

skid steer employs a full line of quick-change attachments; a 44-in.-wide bucket attachment was used for this test. The bucket was wider than the machine, preventing debris from spilling to the side of the bucket and going under the tracks (Strange et al. 2017). The specifications for the Ditch Witch SK850 are shown in Table 3.7.

Figure 3.12. Ditch Witch SK850 mini skid steer.



Table 3.7. Ditch Witch SK850 specifications.

Power (hp)	37
Operating Weight (no attachment) (lb)	3,100
Length with Bucket (in.)	105
Width over Tires (in.)	42
Overall Height (in.)	57
Maximum Travel Speed (mph)	4.7

3.2.2 Diamond-blade saw attachment

Cuts Inc. developed a prototype diamond-blade saw attachment, model SS 4200 HF, which is compatible with the Caterpillar CTLs (Figure 3.13). For this evaluation, 42-in.-diam and 0.22-in.-wide C52 diamond-tipped blades were used on the attachment. The C52 blades used in this test are best for medium hardness aggregate types such as river gravel, crushed gravel or granite, and heavily reinforced concrete. The diamond-tipped blade of the skid-steer attachment requires the use of an external water source to keep the blade from overheating during operation. A 2,000-gal commercial water truck was used as the saw's external water source during the experiment.

Four wheels located on the bottom of the unit can be lifted and not used if necessary. Table 3.8 presents the specifications of the SS 4200 HF

diamond-blade attachment, as measured in the field. The dimensions in the table are with the blade installed on the machine. The length and height dimensions are different when the blade is not on the machine because the top half of the blade housing can be lifted for storage or shipping.

Figure 3.13. Cuts Inc. SS 4200 HF diamond-blade saw attachment on CTL.



Table 3.8. Cuts Inc. SS 4200 HF diamond-blade saw attachment specifications.

Length (in.)	66
Height (in.)	52
Width (in.)	50.25
Weight, without Blade (lb)	980

3.2.3 Backhoe loaders

A JCB 4CX backhoe loader with an HM033T hydraulic breaker was used to break up the damaged concrete. A JCB 3CX backhoe loader with a 24-in.-wide bucket was used for excavating the broken concrete and disturbed underlying material; a breaker for the 3CX model was not available for use during the experiment. The 4CX model is currently JCB's most powerful and largest backhoe loader. The most noticeable difference between the two loaders is that the 4CX model has four large tires that are equal in size, while the 3CX model has two smaller tires in the front and two large tires in the back. The 4CX model also has 25% more horsepower than the 3CX model. The JCB backhoes used in this test are shown in Figure 3.14, and specifications are provided in Table 3.9.

Figure 3.14. JCB 3CX (top) and 4CX (bottom) backhoe loaders.



Table 3.9. JCB 3CX and 4CX backhoe loader specifications.

Specification	JCB 3CX	JCB 4CX
Gross Engine Power (hp)	74	100
Operating Weight (lb)	17,196	17,527
Maximum Travel Speed (mph)	23	23.7
Transport Length (ft)	23.58	19.33
Transport Height (ft)	11.25	12.75
Overall Width with Bucket (ft)	7.67	7.58
Fuel Capacity (gal)	38	42.3

3.2.4 Rammer

A multiquip Mikasa MTX-70 rammer, or jumping jack, was used for compacting when backfilling with cement-stabilized soil, as shown in Figure 3.15. The specifications for the jumping jack are shown in Table 3.10.

Figure 3.15. Multiquip MTX-70 rammer.



Table 3.10. Multiquip MTX-70 rammer specifications.

Height (in.)	39.37
Width (in.)	13.78
Length (in.)	31.02
Fuel Tank Capacity (gal)	0.79
No. of Impacts per Second	10.7 to 11.5
Impact Force (lb)	2,855
Operating Weight (lb)	165.34

3.2.5 Plate compactor

A JPC-80 vibratory plate compactor (Figure 3.16) was used for compaction when backfilling with cement-stabilized soil or geocells filled with granular material. The walk-behind plate compactor weighed 190 lb and produced a centrifugal force of 3,968 lb_f. The plate size was 1.77 ft by 1.38 ft.

3.2.6 Tiller attachment

A Caterpillar LT13B tiller attachment was used on a Caterpillar CTL (Figure 3.17) to mix the cement and soil for backfilling with the cement-stabilized soil. The specifications for the tiller attachment are presented in Table 3.11.

Figure 3.16. JPC-80 vibratory plate compactor.



Figure 3.17. Caterpillar LT13B tiller attachment on CTL.



Table 3.11. Caterpillar LT13B tiller attachment specifications.

Width (in.)	71
Height (in.)	30
Length (in.)	38
Drum Speed (rpm)	127
Weight (lb)	926
Working Depth (in.)	1 to 6

3.2.7 Mid-size rider sweeper

A Tennant S30 rider sweeper (Figure 3.18) was used in the final debris removal task. With a single side brush, the sweeper has a 5.2-ft-wide cleaning path and handles up to 133,660 ft^2 of coverage. The hopper's capacity is 14 ft^3. For crater repairs, the equipment was expected to sweep mainly concrete dust, soil, and small pieces of aggregate or concrete. Specifications of the Tennant S30 are shown in Table 3.12.

Figure 3.18. Tennant S20 mid-size rider sweeper.



Table 3.12. Tennant S30 sweeper specifications.

Power (hp)	24.8
Operating Weight (lb)	3,570
Length (in.)	93
Width (in.)	62.5
Overall Height (in.)	58
Maximum Travel Speed (mph)	15

3.2.8 FOD Boss

Foreign object debris (FOD) removal devices such as the FOD Boss 8 (Figure 3.19) are made to collect debris from the surfaces around airport pavements and construction sites. The FOD Boss 8 was used to assist in the final debris removal task, cleaning mostly concrete dust, soil, and small pieces of concrete or aggregate. The deployed sweep width was 8 ft, and the unit weighed 65 lb with the storage bag. The storage bag was 8 ft 4 in. long and 1 ft in diameter. The towed device raked FOD and caught debris in its pockets, acting much like a sweeper and a dust pan. The manufacturer's recommended speed range is between 4 and 25 mph.

Figure 3.19. FOD Boss 8.



3.2.9 Telehandler screed

The telehandler-operated Autoskreed (ASTH) shown in Figure 3.20 was developed by Nasby Fabrication based on ERDC recommendations. It was lifted via fork pockets and extended across a crater repair with the telehandler's extendable boom. It has a number of leveling adjustments such as jacks, but, typically, it can be adequately leveled by tilting the telehandler forks. The ASTH was outfitted with a spring-loaded travel feature that allowed the screed bar to remain in contact with the pavement surface as the boom extends and rises or falls, depending on its initial angle. Two 12-V electric vibrator motors powered by the telehandler's battery are mounted to the screed bar to facilitate strike-off and finishing.

Figure 3.20. Telehandler-powered ASTH.



In this test, a Genie GTH-1256 AF telehandler was used to operate the ASTH. Specifications are provided in Table 3.13. Note that the ASTH is designed to be compatible with multiple telehandlers and could have also been used with the Caterpillar TL1255D or TL642C telehandlers used during the test.

Table 3.13. Genie GTH-1256 AF specifications.

Maximum Gross Power (hp)	142
Operating Weight (lb)	39,394
Rated Load Capacity (lb)	10,000
Maximum Lift Height (ft)	56
Maximum Forward Reach (ft)	41
Maximum Travel Speed (mph)	15

3.2.10 Deployable volumetric concrete mixer

CemenTech Inc. manufactured a deployable volumetric concrete mixer to be used as part of the lighter and leaner equipment set for crater repairs (Figure 3.21). The aggregate bin, 5 ft wide and 6 ft long, had one piercing point and a 2.5-yd^3 capacity, which was capable of containing two super sacks (1 yd^3 each) of cementitious material. A 250-gal water tank and a 165-gal washout tank were located on the front and back of the machine, respectively.

Figure 3.21. Simplified volumetric concrete mixer – 2.5 yd^3.



The deployable concrete mixer had an overall height of 8.9 ft and is 7.8 ft wide. The length was approximately 28 ft. The mixer was equipped with a spare auger.

3.2.11 Telehandler forklift

A Caterpillar TL642C telehandler forklift (Figure 3.22) was used to transport the 3,000-lb super sacks of pre-blended flowable fill and rapid-setting concrete materials. The machine also maneuvered the super sacks around the repair site and loaded them into the volumetric concrete mixer described in Section 3.2.10. Table 3.14 presents the basic specifications of the telehandler.

Figure 3.22. Caterpillar TL642C telehandler.



Table 3.14. Caterpillar TL642C telehandler specifications.

Power (hp)	100.6
Operating Weight (lb)	21,245
Rated Capacity (lb)	6,500
Lift Height (ft)	42
Length (ft)	18.5
Width (ft)	7.9
Height (ft)	7.8

3.3 Crater repair materials

Flowable fill was used as the backfill material for the traditional RADR set of crater repairs conducted for this experiment. The flowable fill backfill material used in this experiment was Buzzy Unicem Utility Fill 1-Step 750. Polyurethane foam, cement-stabilized silty sand, and geocells filled with sand were used as the nontraditional backfill materials. CTS Rapid Set Concrete Mix® was used as the rapid-setting concrete cap material for all crater repairs during this experiment.

3.3.1 Rapid-setting flowable fill

In general, traditional flowable fill is a low viscosity, grout-like cementitious blend commonly composed of finely ground cement, fine aggregate, and water. Rapid-setting flowable fill utilizes calcium sulfoaluminate cement to provide a much faster set time than that for traditional flowable fill. The dry materials are stored in large 3,000-lb super sacks fashioned from woven geotextile fabric and lined with plastic. The pre-blended material requires only the addition of water to conduct repair activities.

Rapid-setting flowable fill was selected for RADR operations because it can be placed expediently without the need of mixing equipment by using the placement technique known as the "dry method" (Priddy et al. 2013a), as shown in Figure 3.23. In this method and for this experiment, thin 4- to 6-in.-thick lifts of dry material were placed in the excavated repair, and then approximately 40 to 50 gal of water was applied to the surface of each lift and allowed to percolate through the dry material. The material generally provides an unconfined compressive strength of 250 psi after 30 min of cure time and 750 psi after 3 hr of cure time. Post-trafficking investigations typically reveal a California Bearing Ratio (CBR) of approximately 100 percent after 24 hr of cure time.

Figure 3.23. Flowable fill during dry placement method.



3.3.2 Polyurethane foam

Rigid polyurethane foam consists of two components: (1) a polymeric isocyanate compound and (2) a blend of polyol compounds, catalysts,

proprietary additives, and water. The two components are mixed in a 1:1 ratio (by volume) to form a closed-cell expanding foam that rises and sets in approximately 15 min.

The foam product used for the RADR experiment was FOAM-iT! 10 Slow, which is a water-blown, rigid polyurethane designed to expand to approximately six times its initial volume to produce a final density of approximately 10 pcf. This material is formulated with a relatively slow reaction rate for easier handling during large-pour operations. The main benefit of utilizing expanding foam for crater backfill is the significant reduction in material requirements, which reduces the logistical footprint of the repair process. Material reductions are such that 4,500 lb of liquid foam can replace 30,000 lb of backfill soil.

The foam material was dispensed by using a prototype automated foam dispensing system consisting of a set of two hose pumps with removable elements and a touch-screen control panel. The foam liquid components were delivered to and from the pumps by using reinforced polyethylene hoses. A mixing nozzle was used to mix the two components and place the liquid foam mix directly into the crater. Figure 3.24 shows the placement of foam into an excavated repair.

Figure 3.24. Polyurethane foam during placement with dispenser in background.



3.3.3 Silty sand

The soil used in the cement-stabilized backfill was classified as a silty sand (SM) according to the Unified Soil Classification System (USCS) as described in ASTM D2487 (ASTM 2014a). Silty sand was selected since it is one of the most abundantly available soil types (Robinson and Rabalais 1993). The silt was sourced from Vicksburg, MS, as it was not easily accessed near the test site. The silty sand blend was created at the test site by mixing one part silt to three parts sand with a front-end loader. The silty sand was non-plastic (ASTM 2010) and had the grain size distribution (ASTM 2007) shown in Figure 3.25. The material had a specific gravity of 2.7 (ASTM 2014b), and the moisture-density relationship (ASTM 2012) is plotted in Figure 3.26. This graph indicates that the maximum density, 123.7 pcf, occurs at a target moisture content of 10.6%.

Figure 3.25. Silty sand grain size distribution.

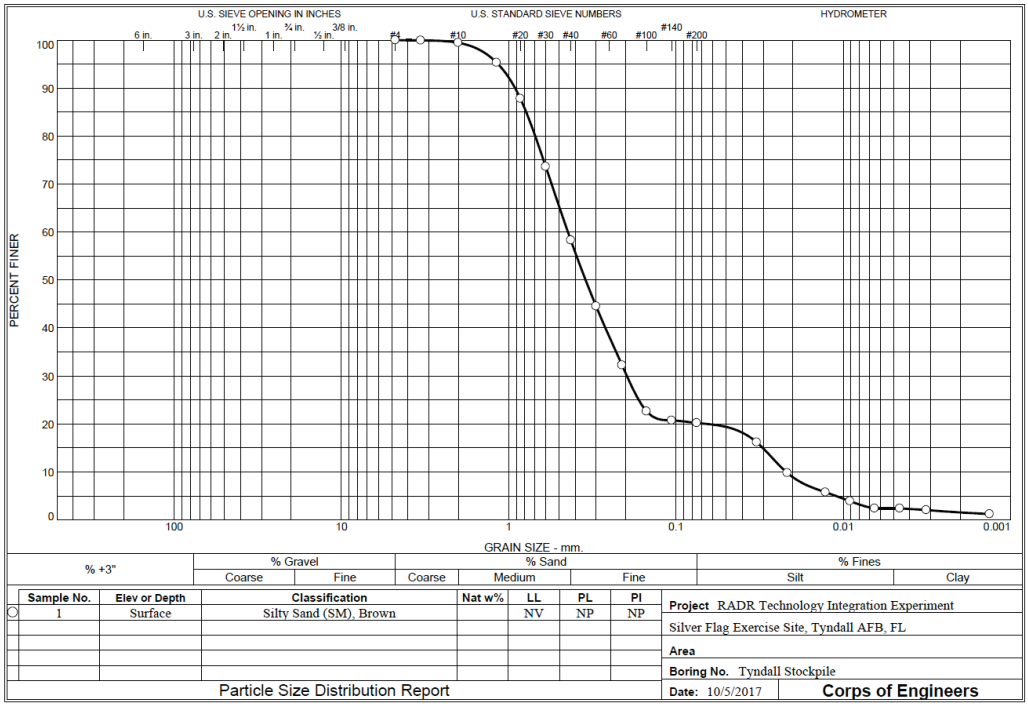
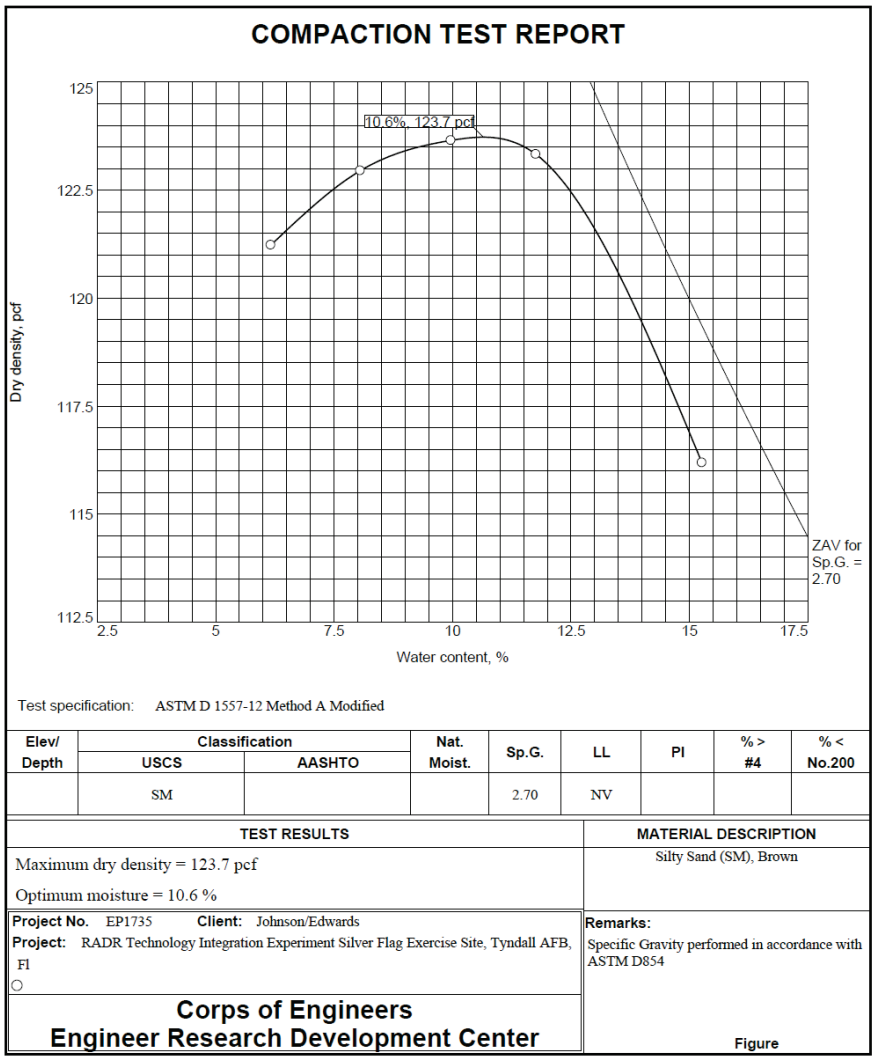


Figure 3.26. Silty sand moisture density relationship.



3.3.4 Portland limestone cement

For the soil stabilization backfill part of the experiment, portland limestone cement (PLC) was used as a stabilization additive for the silty-sand backfill mixture (Figure 3.27). PLC is a combination of calcium silicate-based clinker, limestone, and gypsum and is designated as Type 1L according to ASTM C595 (2018). The PLC was packaged in 92.6-lb bags. The additive was mixed with the soil on a flat surface near the crater repair area. The soil was spread into a 10-ft by 33-ft by 1-ft section, and 12 PLC bags were placed in a grid pattern to evenly disperse the additive to produce a mixture of 5% additive by dry weight.

Figure 3.27. Mixing PLC with silty sand prior to placement in a crater.



3.3.5 Geocells

A geocell, formerly known in the DoD community as “sand grid,” is a geosynthetic cellular confinement system (interconnected cells) used to mechanically reinforce geotechnical materials, mostly cohesionless soils. Within the scope of RADR, geocells are used to reinforce backfill materials for expedient crater repairs. One of the primary benefits of using geocells is that lower quality backfill materials can be used rather than the traditional well-graded crushed limestone material.

For this study, the geocell material was measured and cut to fit in the excavated crater repairs, as shown in Figure 3.28. A needle-punched, nonwoven geotextile fabric was placed on top of the compacted natural subgrade material. The geocell was then placed on top of the fabric, expanded, and held open by using metal stakes at each corner of the repair. Sand was placed in the open cells by using a CTL with a bucket attachment and shovels. The material was compacted by using a vibratory plate compactor. Each geocell was 8 in. high and was installed in two perpendicular lifts, with nonwoven geotextile fabric between the lifts.

Figure 3.28. Geocell material during measuring for cutting.



3.3.6 Rapid-setting concrete

CTS Rapid Set Concrete Mix® is a rigid capping material used in RADR crater repair scenarios because of its high early strength and load-carrying capacity after a minimal curing time of 2 hr. The main cementitious component in the mix is CTS's proprietary Rapid Set Cement®, a calcium sulfoaluminate material. The aggregate within the mix is 3/8-in. maximum size pea gravel.

The dry blend of cementitious material and aggregate is stored in large 3,000-lb super sacks composed of woven geotextile and lined with foil to prevent moisture intrusion. The pre-blended material requires only the addition of water. CTS Rapid Set Concrete Mix® has a fast set time of 20 to 30 min, depending on the ambient air temperature.

The concrete material was mixed and placed by using the simplified volumetric concrete mixer, as shown in Figure 3.29. Bulk citric acid was added to the mix water to increase the working time of the material and to prevent flash setting of material within the mixer. The material is placed in a manner similar to ordinary concrete, but it must be placed expediently since it begins to harden and set within 15 to 30 min. Unlike ordinary PCC, this material can sustain heavy aircraft traffic within 2 hr after placement. CTS Rapid Set Concrete Mix® achieves unconfined compressive strengths in excess of 3,000 psi after 2 hr and over 5,000 psi after 28 days.

Figure 3.29. CTS Rapid Set Concrete Mix® during placement with the simplified volumetric mixer.



4 Traditional RADR Crater Repair Process

The traditional RADR crater repair process consists of eight key tasks conducted by teams of airmen using specific equipment and materials: (1) initial debris removal, (2) hauling, (3) marking, (4) saw-cutting, (5) excavating, (6) backfilling, (7) capping, and (8) final debris removal. The tasks are completed by using the equipment and materials described in Sections 3.1 and 3.3, respectively. Figure 4.1 shows a 9-ft by 9-ft rapid-setting concrete crater repair before cure.

Figure 4.1. Completed rapid-setting concrete crater repair.



The number of teams needed for repairing craters is dependent on the intensity of the attack. Each crater repair team is responsible for 18 small craters. Each repair task is completed by using a set number of team members with the necessary equipment and materials. A crater repair team leader is responsible for accomplishing the repair objective, directing the repair personnel, and ensuring the quality of each repair. The crater team leader typically drives a UTV and transports tools such as shovels, rakes, tape measures, spray paint, brooms, PPE, and utility knives.

The first task in the crater repair process is initial debris removal. The debris removal team begins the crater repair process by clearing the path from the staging area to the minimum operating strip (MOS) and then removing debris from around each crater that is to be repaired. The debris removal team consists of two personnel operating a front-end loader and a CTL with a bucket attachment (Figure 4.2).

Figure 4.2. Debris removal with front-end loader and CTL.



The second task in the RADR process for crater repairs is hauling material. The warehouse operations team is responsible for transporting the repair materials and supplementary equipment from the staging area to the repair site. The primary repair materials requiring dedicated warehouse team assets include the super sacks of rapid-setting flowable fill and rapid-setting concrete, which are hauled from the storage site to the repair site (Figure 4.3). The repair materials and supplementary equipment are loaded onto a tractor-trailer. The warehouse operations team consists of four personnel to operate the tractor-trailer, two telehandlers, and the warehouse forklift.

Figure 4.3. Hauling super sacks of cementitious material.



Once the debris has been removed from around the first crater, the marking team uses line-of-sight stanchions to help identify any upheaval around the crater. The line-of-sight profile measurement devices consist of two sighting stands, or stanchions, placed outside of the upheaved area and a target rod that is systematically moved within the upheaved area to determine where the upheaved pavement begins and ends. Figure 4.4 shows the stanchions being used during a wet weather crater repair test. Once the upheaval has been identified, the marking team paints lines outlining the crater repair area as a guide for the saw-cutting team. The marking team consists of three members.

Figure 4.4. Crater profile measuring using line-of-sight devices.



Saw-cutting begins once the marking team completes its duties. The current saw-cutting protocol calls for CTLs equipped with wheel-saw attachments to cut the upheaval of two craters simultaneously, as shown at a crater repair in Figure 4.5. Each wheel saw-cuts two lines per repair. A walk-behind saw utilizing a diamond blade can be used in locations where dowel bars are present. The saw-cutting team consists of six team members. Four team members operate the CTLs, while two team members are used as spotters for aligning the saws.

The breaking and excavation teams are responsible for breaking up the damaged PCC within the cut crater repair area and removing the disturbed PCC and subsurface material (Figure 4.6), respectively. An excavator with a hammer attachment is used for breaking any large sections of the existing pavement within the repair area, and a second excavator with a bucket

attachment is used for excavating the broken pavement and disturbed underlying material. The excavation team includes two team members to operate the excavators and one person to direct the excavators.

Figure 4.5. Saw-cutting around crater upheaval.



Figure 4.6. Breaking and excavating damaged PCC.



The backfill team is responsible for filling the prepared excavation to the target surfacing depth using material with sufficient bearing capacity to support heavy aircraft operations. Pre-blended rapid-setting flowable fill is the recommended material for backfilling craters in the traditional RADR process. Figure 4.7 shows flowable fill being placed inside a repair using the dry method. Figure 4.8 shows the process of adding water to the flowable fill.

Figure 4.7. Placing rapid-setting flowable fill backfill by using the dry method.



Figure 4.8. Adding water to flowable fill during dry placement method.



Equipment required when placing rapid-setting flowable fill backfill by using the dry method includes one telehandler for transporting the super sacks of flowable fill from the staging area to the excavated hole, a water truck, and assorted hand tools such as rakes, utility knives, shovels, measuring tape, spray paint, and a water flow meter. Four team members make up the backfill team: one person drives and operates the water truck, one person operates the telehandler, and two people use rakes or shovels to evenly spread the material around the excavated repair area.

Concrete capping is the seventh task in the crater repair sequence. The capping team is responsible for placing a level pavement surfacing capable of supporting heavy aircraft operations within the objective time threshold. Rapid-Set Concrete Mix® or hot-mixed asphalt (HMA) can be used as the capping material for crater repairs in the RADR process. The mixing and placement of the rapid-setting concrete mix is conducted by using only the simplified volumetric mixer (Figure 3.4) or appropriate batching and placement equipment for HMA. Figure 4.9 shows a repair being capped with Rapid-Set Concrete Mix® by using the simplified volumetric mixer.

Figure 4.9. Crater repair with Rapid-Set Concrete Mix® using the volumetric mixer.



Seven team members comprise the capping team, including two members from the upheaval marking team who join the capping team after the marking task is complete. For capping, one person is responsible for operating the volumetric mixer, one person drives the vehicle pulling the volumetric mixer, one person drives and operates the water truck, one person operates the screed, and three people serve as helpers who are responsible for spreading the capping material around the area by using shovels or concrete rakes. Once sufficient material has been placed to fill the crater repair, the surface is finished using either the Wyco Screed King or magnesium straight-edge bar as shown in Figure 3.10 and Figure 3.11.

The final task in the RADR crater repair sequence consists of final debris removal. Angle brooms, FOD removal equipment, and vacuum trucks are used to remove any debris remaining from the original damage or the repair process. The PCC or HMA crater caps are allowed to cure or cool, respectively, while the final debris removal is conducted. The final debris removal team is the same as the initial debris removal team and augmented with any available team members as the crater repair sequence is completed.

The results of many full-scale tests of the RADR crater repair process previously described led to the development of an equipment set being deployed to various military airfields. The generic RADR equipment set for crater repairs consists of

1. graders,
2. dozer,
3. loaders,
4. tractors,
5. trailer (60-ton lowboy),
6. vacuum sweepers,
7. tractor-mounted sweepers,
8. warehouse forklift (6,000 lb),
9. trailer (40 ft) - material,
10. extendable boom forklifts (11,000 lb),
11. extendable boom forklift attachment package,
12. dump trucks,
13. wheeled excavators,
14. excavator attachment package,
15. pneumatic rollers,

16. vibratory rollers,
17. water truck (1,500 gal),
18. CTL,
19. CTL attachment package,
20. trailer (40 ft) - attachments,
21. volumetric mixer,
22. water trailer (2,000 gal),
23. asphalt recycler,
24. light carts, and
25. dump truck water skids (1,000 gal).

The RADR equipment set includes an airfield damage repair (ADR) tool trailer for storing and transporting many of the small tools required in the crater repair process. The ADR Tool Trailer contains of over 150 items -- including tools, materials, and small equipment -- needed to perform small and large crater repairs. An Inclement Weather Crater Repair Tool Kit was developed as a supplemental kit to provide additional tools and materials necessary for the repair of craters in wet weather or cold climate conditions (Bell and Tingle 2017).

5 Experiment Training Procedures and Results

5.1 Procedures

The airmen received three days of training on the RADR equipment and backfill placement alternatives before performing the experiment. A half-day of formal training in the classroom describing the details of the RADR process, equipment, and materials was provided before the airmen received hands-on training in the field. In the field, the ERDC staff briefed the repair team again on the crater repair process, equipment, and materials. The majority of the airmen were not familiar with equipment operation. Daily safety briefings were provided to all personnel.

On the second day of training, the airmen were assigned their specific crater repair tasks based on experience and career fields so that they could become familiar with the procedure of their assigned task(s), operating the necessary equipment, and their role in the crater repair process. The airmen were given ample time to practice operating the equipment on the PCC of the training runway. Also, four practice craters were repaired from start to finish with the support of ERDC engineers and technicians so that the equipment sequence and backfill and capping material and procedures could be learned for each of the four repair methods to be tested. The practice improved each team member's skills and knowledge of the crater repair process.

The third day of training consisted of the airmen repairing three craters in sequence, with limited support from ERDC personnel. This training reinforced the crater repair process and helped the airmen understand the urgency required to complete the repairs in the safest and most efficient manner possible. The lighter and leaner equipment set was chosen for the training craters. This equipment set would be used for three of the four full-scale field tests. Geocells were selected as the backfill material, as this method is the most labor intensive backfill process out of the four backfill materials; thus, the additional practice was valuable.

The lighter and leaner crater repair equipment set with geocells as the backfill consisted of

1. initial debris removal – two ride-on mini track loaders,

2. saw-cutting – three CTLs with wheel-saw attachments, one CTL with a diamond-blade saw attachment, and one water truck,
3. excavation – one backhoe with a hammer attachment and one backhoe with a bucket attachment,
4. backfill with geocells – one CTL with a bucket attachment, one front-end loader, and one plate compactor,
5. capping – one small volumetric mixer, one water truck, one telehandler equipped with the ASTH, and one 6K telehandler,
6. final debris removal – one FOD Boss pulled with a UTV and two ride-on sweepers, and
7. hauling – one tractor-trailer, two telehandlers, and one warehouse forklift.

The air temperature during the repairs of the training craters ranged from 78°F to 90°F with mostly sunny skies, and the wind speed was approximately 8 mph. The excavation depth was approximately 22 in. The geocells with sand backfill were 16 in. thick, and the Rapid Set Concrete Mix® cap was 6 in. thick. The parent slab of Training Repair 1 was 16 in. thick, the parent slab of Training Repair 2 was 18 in. thick, and the parent slab of Training Repair 3 was 8 in. thick. The repair sizes for all three craters were approximately 8.5 ft by 8.5 ft. The entire repair process was timed for comparison and for helping the team members understand the need for urgency and efficiency.

5.2 Results

Table 5.1 summarizes the timing results of each individual task during the three-crater repair training sequence. These results give the times that the actual tasks were taking place; they do not include any wait times between tasks (e.g., waiting for the mixer to be loaded, equipment malfunctions, cure times, etc.). Final debris removal was not included in the timing data because the task took place during the required 2-hr curing of the repairs before traffic was applied. The three-crater repair training sequence took 3 hr 47 min to complete (start of initial debris removal on Training Repair 1 to completion of capping on Training Repair 3). This time does not include the 2-hr cure period that would be required prior to opening the pavement to aircraft traffic.

Three wheel saws and one diamond-blade saw were used for cutting around the craters. The average saw-cutting rates of the 18-in.-thick and 16-in.-thick parent slabs using the wheel saws and diamond-blade saw

were 0.82 ft/min and 1.52 ft/min, respectively. The average saw-cutting rates of the 8-in.-thick parent slab using the wheel saws and the diamond-blade saw were 3.2 ft/min and 2.5 ft/min, respectively. The diamond-blade saw attachment performed significantly better in the thicker PCC than the wheel-saw attachments.

Table 5.1. Three-crater repair training sequence timing results.

Training Repair	Time (min)						
	Initial Debris Removal	Stanchions and Marking	Saw-Cutting	Breaking	Excavation	Backfill	Capping
1	3	2	27	12	30	49	12
2	5	2	39	16	51	39	9
3	3	2	20	6	25	45	16
Avg.	**3.7**	**2.0**	**28.7**	**11.3**	**35.3**	**44.3**	**12.3**

The breaking time of Training Repair 2 was the longest because the PCC was thicker (18 in. thick) than the PCC of Training Repairs 1 (16 in. thick) and 3 (8 in. thick). According to the timing results for the PCC breaking of Training Repairs 1 and 3, it took twice as long to break a slab that was twice as thick. Also, the breaking of the PCC likely took longer than normal because there were no craters blown in the pavement; the operator had to break up a fully intact slab. Excavation of Training Repair 2 was longer than the other training craters because the operator had trouble excavating the broken PCC at the corner where the two cuts had been made with the diamond-blade saw attachment. The backhoe with the breaker attachment had to return to Training Repair 2 to finish breaking up the corner of the excavation. The additional breaking, however, lasted only 1 min.

The backfill team cut the geocells to the correct sizes while the breaking and excavation tasks were being completed. The crater team leader relayed the exact repair dimensions to the backfill team after the saw-cutting task was completed on each repair. It took approximately 20 min for the backfill team to install each layer of geocells for a total average backfill time of 44 min. The repairs consisted of two 8-in.-thick layers of geocells filled and compacted with sand. Geotextile was placed on top of the existing compacted subgrade and between the two layers of geocells. The two layers of geocells were placed perpendicular to one another to ensure that the joints did not align.

The 6-in.-thick rapid-setting concrete cap for each training crater repair was completed at an average time of approximately 12 min. Training Repair 3 took 16 min for capping. The mixer ran out of the rapid-setting mix during capping due to miscommunication of the capping and warehouse teams. It took 2 min to reload the mixer's bin. Otherwise, the capping could have been completed in 14 min.

Final debris removal using the FOD Boss and the two ride-on sweepers was not timed. The final debris removal task took place while the crater repairs were curing. The FOD Boss was not effective for the final debris removal task. The device was filled with the concrete dust and debris after just one sweep of the area. Thus, the FOD Boss should not be used until a majority of the loose debris has been removed from the pavement surface.

6 Test Procedures and Results

Four full-scale tests were completed using the crater repair equipment and backfill materials described in Chapter 3. Each test was conducted on separate days and consisted of a timed five-crater repair sequence. Test #1 included using the lighter and leaner equipment set with rapid-setting flowable fill as the backfill material. Tests #2 and #3 used the lighter and leaner equipment set and polyurethane foam backfill and cement-stabilized silty sand backfill, respectively. The traditional crater repair equipment set and geocells with sand backfill were used for Test #4. All 20 repairs were capped with 10 in. of Rapid Set Concrete Mix®.

Twenty simulated craters (five craters for each test) were created on the training runway by using C4 explosives during a previous project. Additional concrete debris was scattered around the simulated craters before each test to create a more realistic environment (Figure 6.1). After training, the team of 28 airmen completed the repairs with no assistance from ERDC personnel.

Figure 6.1. Typical debris field created for each test.



The airmen gathered all necessary personal protective equipment, tools, and supplies immediately prior to the start of each test. Fuel levels of the equipment were also checked. The equipment operators lined up their equipment along the staging area in process order, beginning with the initial debris removal team and the crater team leader and ending with the capping team. The preparation and staging of equipment would be

conducted while the damage assessment and UXO clearance tasks are being completed under the RADR concept of operations. The timed repair process began as soon as all team members were ready; each test preparation took approximately 20 to 30 min.

6.1 Test #1: Lighter and leaner equipment; rapid-setting flowable fill backfill

6.1.1 Procedure

The test evaluating the crater repair process using the lighter and leaner equipment set and rapid-setting flowable fill as the backfill material was conducted on 27 August 2017. The weather during the test consisted of an 8-mph wind, partly cloudy skies, and air temperatures that increased from 77°F to 87°F.

The lighter and leaner RADR equipment set consisted of two Ditch Witch SK850 mini track loaders for the initial debris removal task (Figure 6.2). The two mini track loader operators worked continuously throughout the repair process to clean around the repair areas and push debris away from the repair area.

Figure 6.2. Debris removal with Ditch Witch SK850 mini track loaders.



No specialized equipment, other than stanchions used to identify any pavement upheaval, was needed for the upheaval marking team. The marking team, comprised of three airmen, used a 10-ft-long aluminum beam as a straightedge for spray-painting a “square” around the upheaval.

The painted lines served as a guide for the saw-cutting team. This process was identical to that described in Chapter 4.

The saw-cutting team used three Caterpillar 289D XPS CTLs and one Caterpillar 279D XPS CTL. One of the 289D models was equipped with the Cuts Inc. SS 4200 HF diamond-blade saw attachment, and the other CTLs were equipped with the Caterpillar SW360B wheel-saw attachments. A 2,000-gal commercial water truck supplied water to the diamond-blade saw. Due to the restricted number of airmen, an ERDC employee served as the water truck operator. One of the two saw spotters was responsible for hooking up the water hose to the diamond-blade saw once the saw was aligned. One wheel saw and the diamond-blade saw worked simultaneously beginning with Repair 1, while the other two wheel saws started cutting on Repair 2. The two saw spotters worked to clear sawdust from the marked lines by using shovels and brooms during the cutting task. The saws continued cutting around the craters in sequence, where needed. Figure 6.3 shows a wheel saw and the diamond-blade saw-cutting around a crater with the water truck for the diamond-blade saw in the background.

Figure 6.3. Wheel saw and diamond-blade saw in operation.



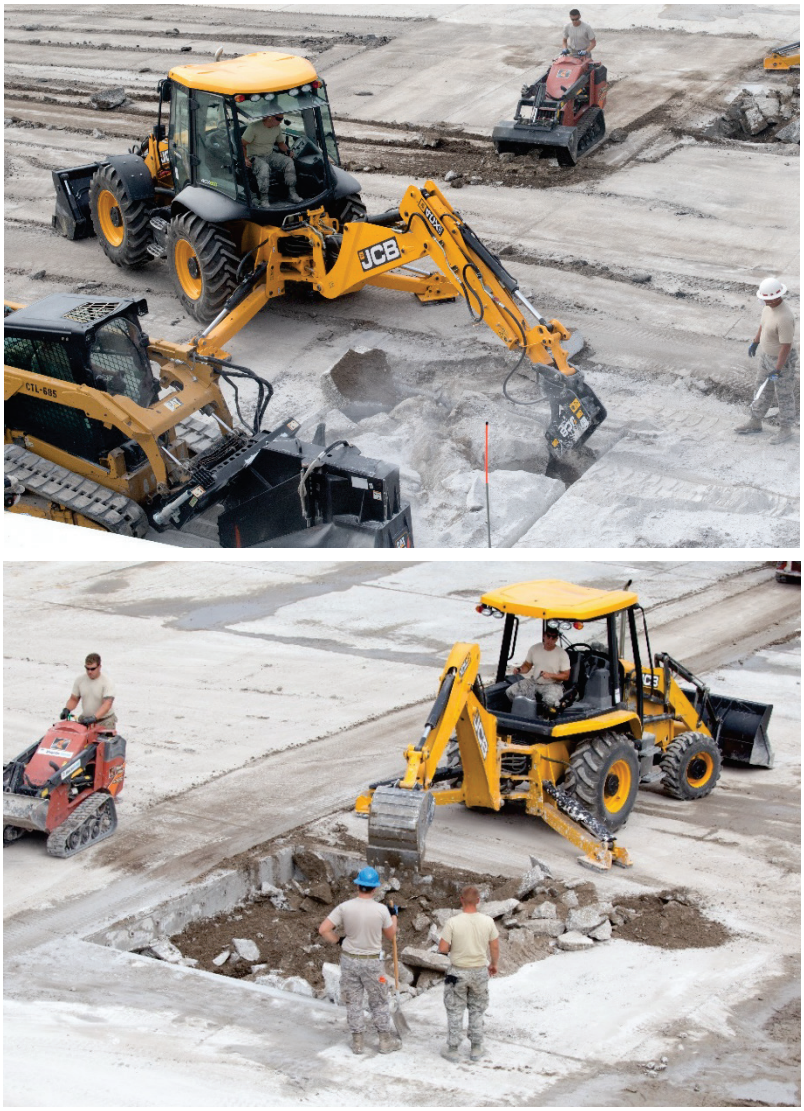
Before the test, the warehouse team began loading super sacks of flowable fill and Rapid Set Concrete Mix® from the warehouse tent and onto the tractor-trailer. After the completion of the saw-cutting task, the warehouse team began hauling and unloading the super sacks of flowable fill and Rapid Set Concrete Mix® from the tractor-trailer to the repair areas, using one Caterpillar TL642C telehandler and one Caterpillar TL1255D telehandler. The super sacks were staged strategically so that they were convenient for

the backfill and capping tasks. Four team members were used to operate the tractor-trailer, two telehandlers, and the warehouse forklift.

The excavation task, which began as soon as saw-cutting on Repair 1 ended, was completed by using a JCB 4CX backhoe with a HM033T hammer attachment and a JCB 3CX backhoe with a 24-in.-wide bucket attachment. The backhoe with the hammer attachment broke the concrete inside the cut repair area into approximately 3-ft-size pieces; then the backhoe with the bucket attachment removed the broken PCC and disturbed soil 24 in. deep from the top of the repairs (Figure 6.4). A spotter assisted the excavation team with breaker and bucket placement and was responsible for keeping up with the depth of soil and PCC removal. The spotter also marked small lines with spray paint along the repair walls at 10 in. from the top of the repairs to delineate the target cap thickness. This procedure helped the backfill team gauge how much material was needed when backfilling.

Backfilling with the rapid-setting flowable fill consisted of placement of the dry pre-blended material in the prepared crater using a CAT TL642C telehandler and activating the hydration process by wetting the material. The warehouse team, or haul team, prepositioned super sacks of rapid-setting flowable fill near the repair area after the saw-cutting task. Using utility knives, backfill team members sliced open the bottom of one bag of flowable fill, which was held over the repair area with the telehandler. The material was spread around the excavated repair using shovels and rakes. Approximately 50 gal of water was then metered on the surface and allowed to percolate through the dry material. The process was repeated until the backfill material reached the paint lines marked by the excavation spotter to leave room for capping. The backfill thickness for each repair was 14 in. Each of the five repairs needed 3 to 5 super sacks of flowable fill, depending upon the actual repair size. The backfill team included the water truck operator, the telehandler forklift operator, and two helpers. This process and the backfill process described in Chapter 4 were identical with the exception that a smaller 6,000-lb capacity telehandler was used instead of the 10,000-lb capacity telehandler included in the traditional RADR equipment set.

Figure 6.4. Breaking and excavating with JCB 4CX (top) and 3CX (bottom).



The final task in the timed crater repair process was to cap each repair with 10 in. of Rapid Set Concrete Mix®. The capping team included a military vehicle driver for pulling the small volumetric mixer, an operator for the small volumetric mixer, an operator for the Genie GTH-1256 AF telehandler with the screed attachment, an operator for the water truck, an operator for the Caterpillar TL642C telehandler used for keeping the mixer loaded with capping material, as shown in Figure 6.5, and two helpers using shovels and concrete rakes to move the rapid-setting material around the repair. The water truck was positioned to keep the mixer well-supplied. Two team members, the water truck operator and a helper, were from the marking team. They joined the capping team after the upheaval marking team's duties were finished.

Figure 6.5. Caterpillar TL642C loading small volumetric mixer.



The capping process for each repair began approximately 30 min after the completion of the backfill task. Repairs 1 and 2 each received two passes with the ASTH once the capping material was flush with the parent slab (Figure 6.6). The small volumetric mixer malfunctioned prior to capping Repair 3. A 3,000-lb super sack of Rapid Set Concrete Mix® was dropped onto a hydraulic fitting due to an error by a telehandler operator. The larger volumetric mixer from the traditional RADR equipment set was also inoperable at the time. Therefore, the capping of Repairs 3, 4, and 5 were not completed. The timing data from the repair process were stopped after the capping of Repair 2. Repairs 1 and 2 used approximately 5 and 10 super sacks of the rapid-setting concrete, respectively. The large difference in the number of super sacks was due to the repair sizes.

Figure 6.6. Screeding crater repair with telehandler-operated ASTH.



The final debris removal was completed with the same personnel used for initial debris removal. This task was not timed because it was completed during the 2-hr cure period for the Rapid Set Concrete Mix® caps. The lighter and leaner equipment used for the final debris removal task included the FOD Boss 8, which was pulled with a UTV, and two Tennant S30 vacuum sweepers (Figure 6.7). The final debris removal equipment worked to clean the concrete dust and small aggregate from around the repairs.

Figure 6.7. Typical final debris removal with lighter and leaner equipment.



After the repairs were capped, test data -- including surveying, heavy weight deflectometer (HWD) testing (Figure 6.8), and visual inspection -- were collected to characterize the condition and capacity of the completed repairs. The HWD data gave the impulse stiffness modulus of the pavement structure as an indicator of the structural capacity of the repair.

Figure 6.8. HWD testing of crater repair.



All capped repairs, Repairs 1 and 2, were trafficked 2 hr after capping with 112 passes (28 coverages) of an F-15E single-wheel load cart (Figure 6.9) in a normally distributed wander pattern. This pass level represents seven traffic patterns of the F-15E aircraft. The repair with the most noticeable damage, Repair 2, was trafficked further until 3,504 passes or 876 coverages, which is the sustainment repair target pass level, or failure was achieved. Failure for this experiment was defined as a repair posing as a tire hazard, a high-severity shattered slab, or a slab containing a spall that was at a minimum 24 in. long, 6 in. wide, and 2 in. deep. Data were collected at periodic intervals during trafficking.

Figure 6.9. F-15E single-wheel load cart.



Data collection was completed on Repair 2 after the completion of trafficking. This included surveying the surface to check for elevation changes, performing HWD tests to estimate layer stiffness, extracting three cores from the repair to validate cap thickness, conducting two DCP tests on the rapid-setting flowable fill via drilled holes to estimate the backfill material's CBR, and visually inspecting the repair surface for pavement distresses. The extracted cores were also tested at ERDC to measure the Rapid Set Concrete Mix®'s 28-day ultra-compressive strength.

6.1.2 Results

The timed crater repair event started at 0815 and ended at 1217 for a total time of 4 hr 2 min. The backfilling of Repair 5 was completed at 1217; the small volumetric mixer broke during the test, so Repairs 3, 4, and 5 were not capped. The PCC parent slab characteristics and the crater repair timing results are shown in Table 6.1. The Tactics, Techniques, and Procedures (TTP) manual, developed by the U.S. Air Force (Air Force Civil

Engineer Center 2016), serves as the unofficial expeditious process for airfield recovery after a major attack. The TTP times shown in Table 6.1 were developed with the traditional RADR crater repair equipment and with rapid-setting flowable fill as the backfill material; therefore, a comparison of the time difference between the two equipment sets was available. The TTP times shown are also for small crater repairs that are typically 8.5 ft by 8.5 ft (72 ft²) and 18 in. thick. Repairs 1, 3, 4, and 5 ranged in size from 105 ft² to 121 ft², while Repair 2 had an area of 176 ft².

Table 6.1. Repair characteristics and task times for Test #1 (lighter and leaner equipment and flowable fill backfill).

Repair			Time (min)						
No.	Area (ft²)	Parent Slab Thickness (in.)	Initial Debris Removal	Upheaval Marking	Saw-Cutting	Breaking	Excavation	Backfill	Capping
1	117	16	1	1	25	3	43	36	24
2	176	unknown	2	1	42	7	48	44	30
3	105	12	1	2	32	10	33	20	----
4	116	10	2	1	37	11	57	28	----
5	122	13	1	1	28	17	77	22	----
Average Time			1.4	1.2	32.8	9.6	51.6	30	27
TTP	72	18	1.5	4.5	22	12	11	30	35

The times associated with excavating the PCC debris and soil by using the JCB backhoe were three to seven times slower than the goal written in the TTP when using the traditional wheeled excavator. This delay was due to several reasons: (1) the crater repair sizes were larger than those described in the TTP, (2) the backhoe operator was a little slower than necessary due to trying to make the excavations perfectly clean, (3) sometimes the diamond-blade saw did not create enough of an overcut at the ends of each cut, locking the corner, and (4) the backhoe had to reposition two to three times at each crater repair. Often times, the JCB backhoe used for breaking provided some minor assistance to the JCB backhoe used for excavation.

The initial debris removal, upheaval marking, breaking, backfill, and capping times completed with the lighter/leaner equipment were comparable with the traditional RADR crater repair equipment, as indicated with the TTP goals. Overall, the saw-cutting times using the three wheel saws and one diamond-blade saw were comparable or better,

given the increase in the repair areas as compared with the typical area given in the TTP.

The saw-cutting and excavation tasks were the slowest in the crater repair process for this experiment. The saw-cutting rate goal in the TTP is 1 ft/min. The saw-cutting rates for the four cuts associated with each crater repair for Test #1 are shown in Table 6.2.

Table 6.2. Saw-cutting rates for Test #1.

Repair No.	Saw Type[a]	Cut Length (in.)	Cut Time (min)	Cut Rate (ft/min)
1 (16 in. thick)	WS, DB[b]	166	12	1.15
	DB	151	7	1.80
	WS	163	8	1.70
	DB	157	7	1.87
2 (thickness unknown)	WS	178.5	23	0.65
	WS	205.5	14	1.22
	WS	186	15	1.03
	WS	166	14	0.99
3 (12 in. thick)	WS	155	9	1.44
	DB	133	5	2.22
	WS	159	11	1.20
	DB	166	8	1.73
4 (10 in. thick)	WS	158	12	1.10
	DB	172	8	1.79
	DB	140	7	1.67
	WS	153	18	0.71
5 (13 in. thick)	DB	149	8	1.55
	WS	170	12	1.18
	WS	182	14	1.08
	DB	164.5	8	1.71

[a] WS = Caterpillar SW360B wheel saw; DB = Cuts Inc. SS 4200 HF diamond-blade saw

[b] Both saws used due to steel reinforcement found in PCC

The rates for the SW360B wheel saws ranged from 0.65 ft/min to 1.70 ft/min, depending on the thickness and strength of the PCC. The rate of 1.70 ft/min measured from Repair 1 is atypically fast for a wheel saw in 16-in.-thick PCC. It is unknown whether there was an error in measuring the length of the cut. The wheel saw is the same saw-cutting equipment used for repairing craters by using the traditional method.

The rate for the Cuts Inc. SS 4200 HF diamond-blade saw ranged from 1.55 ft/min to 2.22 ft/min. In general, the diamond-blade saw attachment's cut rate for each repair was over 1.5 times faster than the cut rates of the wheel-saw attachments.

The first cut for Repair 1 began by using the wheel saw; however, the wheel saw had difficulty cutting through the PCC. It was determined that the location on that side of the slab had steel dowels; therefore, the diamond-blade saw was used to finish the cut. The diamond-blade saw had no problems cutting through the steel.

A Gantt chart for the Test #1 repairs is shown in Figure 6.10. The Gantt chart provides a timeline overview of the entire experiment, including the wait times between each crater repair task. The overlap between some of the crater repair tasks can also be viewed in the Gantt chart. Many times, the breaking task would begin on a repair before the saw-cutting process was complete. The breaking team was often waiting on the saw-cutting team after breaking each repair. The crater damage was broken up into smaller pieces than necessary because the operator had time due to waiting on the saw-cutting teams, thus producing an artificially longer breaking task time.

Also, the Gantt chart shows that the excavation task was occurring simultaneously on the repairs. During this process, the operator of the backhoe with the hammer attachment would use the bucket at the front of the machine to remove broken debris from the opposite side of the repair being excavated by the removal team. The entire crater repair process for this test (initial debris removal of Repair 1 to the backfilling of Repair 5) was 242 min.

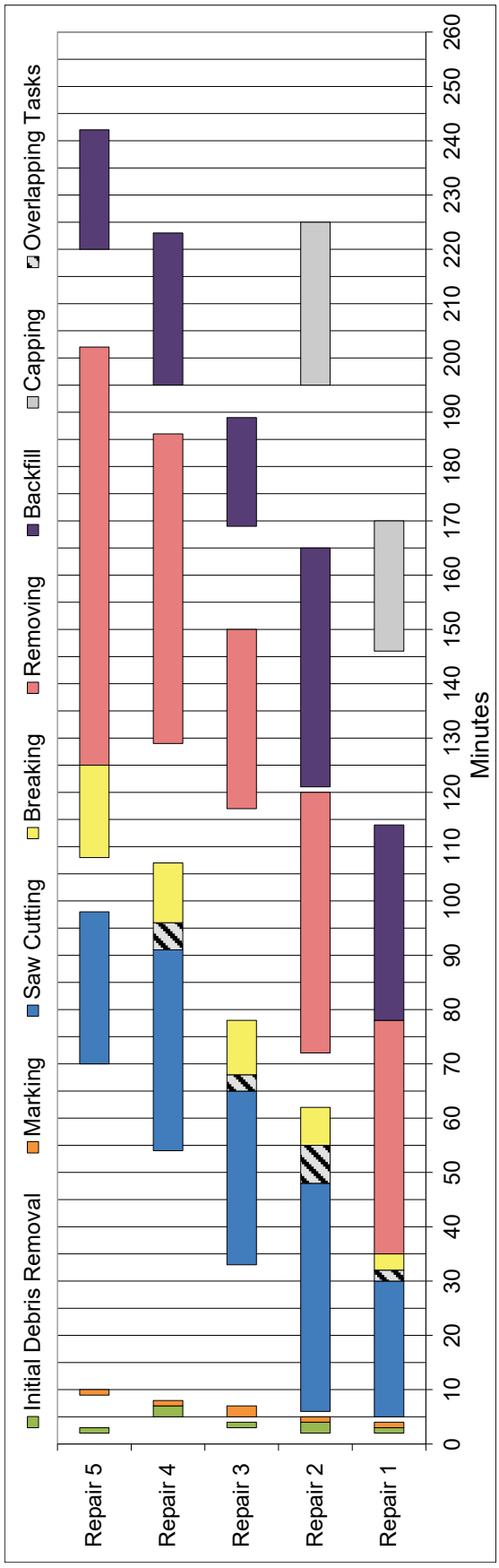


Figure 6.10. Gantt chart of overall progress with lighter and leaner crater equipment and flowable fill backfill (Test #1).

The airmen were able to operate the majority of the lighter and leaner equipment without significant issues. However, the airmen had difficulty operating the deployable mixer. This was likely due to it being the first time the airmen operated the mixer without assistance or guidance from ERDC personnel. The mixer controls are simplified, but small adjustments must be made by an experienced operator to ensure the correct water-cement ratio is used and that the bin is supplied with enough material to continuously push the dry concrete to the auger.

The deployable volumetric mixer holds slightly more than two of the 3,000-lb super sacks (1 yd^3 each) of cementitious material. During the capping operation, it was noticed that a large amount of the dry material was leaking from the dry-material bins and onto the concrete below (Figure 6.11). This was due to failure to attach a rubber flap during manufacturing. The airmen had difficulty keeping the dry-material bins full due to both the leak and the relatively small size.

The surface of Repairs 1 and 2 displayed shrinkage cracks soon after the caps were placed (Figure 6.12). This was likely due to the capping material being too wet at the surface. Repairs 1 and 2 were trafficked with 112 passes (28 coverages) of the F-15E load cart 2 hr after Repair 2 was capped. Repair 1 was then selected for further trafficking. After 1,056 passes (264 coverages) with the F-15E load cart, low-severity cracks began forming in one area of the wheel path on the south transverse joint. The repair did not show any additional visible surface distresses until 3,504 passes (876 coverages), which is when trafficking was ceased. The pass level of 3,500 represents a sustained repair. The low-severity cracks that were on the south transverse joint formed a low-severity joint spall (Figure 6.13). Overall, the repair performed well under the simulated F-15E traffic and did not reach failure before the target pass level of 3,504 passes (876 coverages) was achieved.

Figure 6.11. Pile of dry material spilled from small volumetric mixer bin.



Figure 6.12. Shrinkage cracking on surface of Repair 1 (flowable fill backfill) before trafficking.



Figure 6.13. Low-severity joint spalling on Repair 1 (flowable fill backfill) after 3,504 passes.



Repair 1 was tested five times throughout trafficking by using the HWD to measure the stiffness of the repaired pavement structure. The stiffness measurements did not follow a trend with increasing passes, which was not unusual. The stiffness data ranged from 1,200 kips/in. to 5,000 kips/in. and averaged 1,300 kips/in. The 5,000 kips/in. was a spike in the data after 112 passes (28 coverages). The 1,200 kips/in. measurement was taken before trafficking, and 3,500 kips/in. was measured after 3,504 passes (876 coverages).

Repair 1 was surveyed for surface elevation changes before, during, and after trafficking. The data showed a maximum elevation change of 0.38 in. at one location on the centerline of the repair and 0.50 in. at one location on the repair's cross section.

6.2 Test #2: Lighter and leaner equipment; polyurethane foam backfill

6.2.1 Procedure

Test #2 was designed to evaluate the crater repair process using the lighter and leaner equipment set and polyurethane foam as the backfill material. Test #2 was conducted on 28 August 2017 with 7-mph winds, clear skies, and air temperatures that increased from 75°F to 86°F throughout the test.

The same lighter and leaner equipment and repair procedures described in Section 6.1.1 were used for this test. However, the large simplified volumetric mixer included in the traditional RADR crater repair equipment set was used for capping since the deployable mixer was inoperable. The only major difference between Test #1 and Test #2 was the backfill material and placement method used. Backfilling the craters with the polyurethane foam consisted of using a prototype automated foam distribution system, identified as Containerized Rapid Airfield Damage Repair Prototype 1 Lightweight (CRADR1-L), as shown in Figure 6.14, to dispense liquid foam material into the excavated repair and then allowing the foam to expand and set before the rapid-setting concrete cap was applied.

Figure 6.14. Prototype automated foam dispensing system with foam totes.



For this test, the backfill team consisted of four airmen, including the automated foam distribution system operator, the nozzle operator, and two helpers. Before the test started, the warehouse team prepositioned two sets of liquid foam component totes on the same trailer that carried the foam dispenser. The foam backfill process (Figure 6.15) for each repair was as follows.

1. The excavated repair dimensions were measured by the backfill team and entered into the automated foam distribution system through the touch-screen control panel. The required measurements, in inches, were the total width, length, and depth of the repair, as well as the desired surface cap thickness.
2. The bottom of the excavation was lined with 10-mil polyethylene plastic sheeting, making sure that the liner was in contact with the excavation walls and corners. Rebar was installed into the soil walls and corners to pin and hold the liner in place.
3. The foam dispenser was set up by following the procedures indicated in the user's manual. The liquid polyurethane foam mix was dispensed in approximately 4 to 6 min, depending on the repair volume. Once the total liquid volume required was dispensed, the foam dispenser was moved to the next excavated repair.
4. The foam was allowed to expand and cure for about 10 min. At that point, the excess liner above the foam backfill was cut and removed. When the foam expanded in each excavated repair, an uneven and cracked domed surface was formed (Figure 6.15[f]). Therefore, the foam surface of each repair was inspected to identify areas that required leveling or cutting so that enough room was provided for the required 10-in. rapid-setting concrete cap thickness. The dome shape in Repairs 1, 2, 4, and 5 had to be trimmed so that the cap thickness would still be 10 in. in the middle of the repair. These domed areas were cut with a reciprocating saw, and the excess material was discarded by the debris removal team.

Figure 6.15. Overview of foam backfill process in Test #2.



The target foam backfill thickness was 14 in. However, since the expanded foam backfill surfaces were uneven, the backfill thicknesses varied throughout the repair. One set of liquid foam totes (one tote per component) was enough to backfill the first two repairs. The material

transfer hoses on the foam dispenser were swapped from the empty totes to the new totes after Repair 2 was backfilled. Generally, one set of totes (275 gal per tote) is enough to backfill three small (8.5 ft by 8.5 ft) crater repairs. However, repair dimensions varied during this test.

The final task in the timed crater repair process was to cap the five repairs with 10 in. of Rapid Set Concrete Mix®. The capping process for each repair began after approximately 10 to 25 min from the completion of the backfill task. The capping team and procedures were the same as described in Section 6.1.1 except that the larger 7-yd^3 simplified volumetric mixer was used.

The final debris removal task, which was not timed, was completed with the same personnel who completed the initial debris removal task. The equipment used for cleaning the concrete dust and small aggregate from around the repairs included two mini ride-on sweepers. The FOD Boss was also used.

The five repairs were surveyed to provide an elevation baseline and were visually inspected for surface distresses shortly before trafficking began after the 2-hr cure time. Also, the HWD was used at the center of each repair to identify the stiffness of each pavement structure before trafficking. All capped repairs were trafficked in a normal distribution with 112 passes (28 coverages) of the F-15E single-wheel load cart 2 hr after capping Repair 5. The same data collection routine was repeated for each repair after 112 passes (28 coverages).

Repair 2, which had the most initial damage, was trafficked further until 3,504 passes (876 coverages) or failure was achieved. Failure for this experiment was defined as a repair posing as a tire hazard, a high-severity shattered slab, or a slab containing a spall that was at minimum 24 in. long, 6 in. wide, and 2 in. deep. Surface damage was monitored throughout trafficking.

Post data collection was completed on Repair 2 after trafficking. This included surveying the surface to check for elevation changes, performing HWD tests to estimate layer stiffness, extracting three cores from the repair to validate cap thickness, conducting two DCP tests on the foam via the drilled holes to estimate the backfill material's CBR, and visually inspecting the repair surface for pavement distresses. The extracted cores

were tested at ERDC to measure the Rapid Set Concrete Mix®'s 28-day ultra-compressive strength.

6.2.2 Results

The timed crater repair test started at 0835 and ended at 1322. The PCC parent slab characteristics and the crater repair timing results are shown in Table 6.3. The TTP times shown in Table 6.3 were based upon the traditional RADR crater repair equipment and with rapid-setting flowable fill as the backfill material; therefore, a comparison of the time difference between the two equipment sets and backfill materials was available. The TTP times shown are also for small crater repairs that are typically 8.5 ft by 8.5 ft (72 ft²) and 18-in.-thick concrete pavements. Repairs 1, 3, and 4 were smaller, ranging in size from 46 ft² to 75 ft², while Repairs 2 and 5 had larger areas of 129 ft² and 147 ft², respectively.

Table 6.3. Repair characteristics and task times for Test #2 (lighter and leaner equipment and foam backfill).

Repair			Time (min)						
No.	Area (ft²)	Parent Slab Thickness (in.)	Initial Debris Removal	Upheaval Marking	Saw-Cutting	Breaking	Excavation	Backfill	Capping
1	75	8	1	1	16	2	26	15	26
2	129	unknown	2	2	21	4	38	19	27
3	58	17	2	3	18	19	36	19	33
4	46	17	4	2	23	8	19	13	10
5	147	17	5	3	34	24	83	36	34
Average Time			2.8	2.2	22.4	11.4	40.4	20.4	26.0
TTP	72	18	1.5	4.5	22	12	11	30	35

The initial debris removal times for Repairs 2, 3, 4, and 5 were longer than necessary because of the technique the team used. The team made multiple parallel passes in a row, clearing parts of the debris from all five crater repairs with each pass instead of cleaning the debris around one crater at a time. The upheaval marking, saw-cutting, breaking, backfill, and capping tasks met or exceeded the goals described in the TTP. The PCC parent slabs in this set of tests appeared to be weak because the concrete would somewhat crumble during the breaking task, which would explain why the saw-cutting and breaking times were so fast, considering

the repair sizes. However, the times associated with excavating the PCC debris and soil when using the JCB backhoe were slower than the goal written in the TTP, which is based upon the traditional large wheeled excavator. The excavation task was the weak link for this repair process. Backfill times were improved by using the foam technology as compared to the traditional rapid-setting flowable fill backfill.

The saw-cutting rate goal in the TTP is 1 ft/min. The saw-cutting rates for the four cuts associated with each crater repair are shown in Table 6.4. The rates for the SW360B wheel saws ranged from 0.88 ft/min to 3.22 ft/min, depending on the thickness and strength of the PCC. The wheel saw is the same saw-cutting equipment used for repairing craters with the traditional RADR method. The rate for the Cuts Inc. SS 4200 HF diamond-blade saw ranged from 1.05 ft/min to 3.32 ft/min. Overall, the diamond-blade saw attachment's cut rate for each repair was faster than the cut rate of the wheel-saw attachment.

The third cut for Repair 1 began by using the wheel saw; however, the wheel saw had difficulty moving through the PCC. It was determined that that side of the slab had steel reinforcement; therefore, the diamond-blade saw was used to finish the cut. The diamond-blade saw had no problems cutting through the steel.

A Gantt chart for the repairs is shown in Figure 6.16. The Gantt chart provides a timeline overview of the entire test, including the wait times between each crater repair task. The wait time between excavation and backfill for Repair 1 was because the backfill team waited until the excavation was completed in Repair 2 so that Repairs 1 and 2 could be backfilled successively. The wait times between the foam backfill tasks of Repairs 2 and 3, 3 and 4, and 4 and 5 were because the backfill team had no need for urgency due to the slow operation of the excavation task.

Overlap between saw-cutting and breaking can also be viewed in the Gantt chart. For Repair 2, the breaking task began before the saw-cutting process was complete. Also, the backhoe operator assigned to breaking would begin the removal process of the following repair (Repairs 3, 4, and 5) while the backhoe operator assigned to excavation worked a previous repair. Furthermore, the capping team would begin using the mixer for material placement on a following repair while part of the team stayed behind to complete concrete finishing on a previous repair. The mixer's auger was briefly washed out after Repairs 2 and 4. The entire crater repair process for this test was 287 min.

Table 6.4. Saw-cutting rates for Test #2.

Repair No.	Saw Type[a]	Cut Length (in.)	Cut Time (min)	Cut Rate (ft/min)
1 (8 in. thick)	WS	116	3	3.22
	DB	125.5	8	1.31
	WS/DBb	137	5	2.28
	DB	119.5	3	3.32
2 (thickness unknown)	WS	147	8	1.53
	WS	141	9	1.31
	WS	172	11	1.30
	WS	164	8	1.71
3 (17 in. thick)	DB	106	4	2.21
	DB	107	5	1.78
	WS	110.5	8	1.15
	DB	118	4	2.46
4 (17 in. thick)	WS	92.5	6	1.28
	WS	95	9	0.88
	WS	100	9	0.93
	WS	92	6	1.28
5 (17 in. thick)	DB	151	12	1.05
	DB	147	5	2.45
	WS	169	13	1.08
	DB	167	8	1.74

[a] WS = Caterpillar SW360B wheel saw; DB = Cuts Inc. SS 4200 HF diamond-blade saw

[b] Both saws used due to steel reinforcement found in PCC

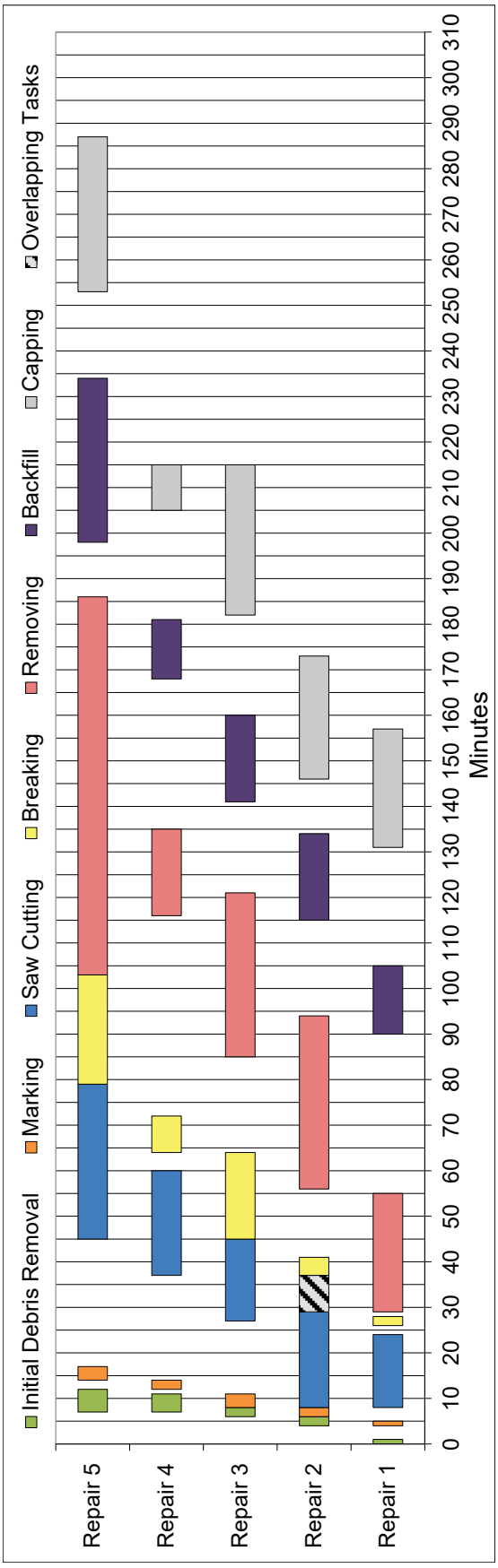


Figure 6.16. Gantt chart of overall progress with lighter and leaner crater equipment and foam backfill (Test #2).

The surface of Repairs 1, 2, 3, and 5 exhibited shrinkage cracks soon after the caps were placed (Figure 6.17), likely due to the capping material being placed too wet. All repairs were successfully trafficked with 112 passes (28 coverages) of the F-15E load cart 2 hr after Repair 5 was capped, and no additional surface distresses were observed. Repair 2 was then selected for further trafficking since the repair exhibited the largest amount of shrinkage cracks on the surface. After 1,056 passes (264 coverages), low-severity linear cracks began forming in one area of the wheel path on the north and south joints. Also, two low-severity linear cracks began forming transverse to the traffic direction across the repair. The repair did not show any additional visible surface distresses until 3,504 passes (876 coverages). The low-severity cracks that were on the north and south transverse joints became medium-severity joint spalls, as shown in Figure 6.18. Overall, the repair performed well under simulated F-15E traffic.

Figure 6.17. Shrinkage cracks on Repair 2 with foam backfill (Test #2).

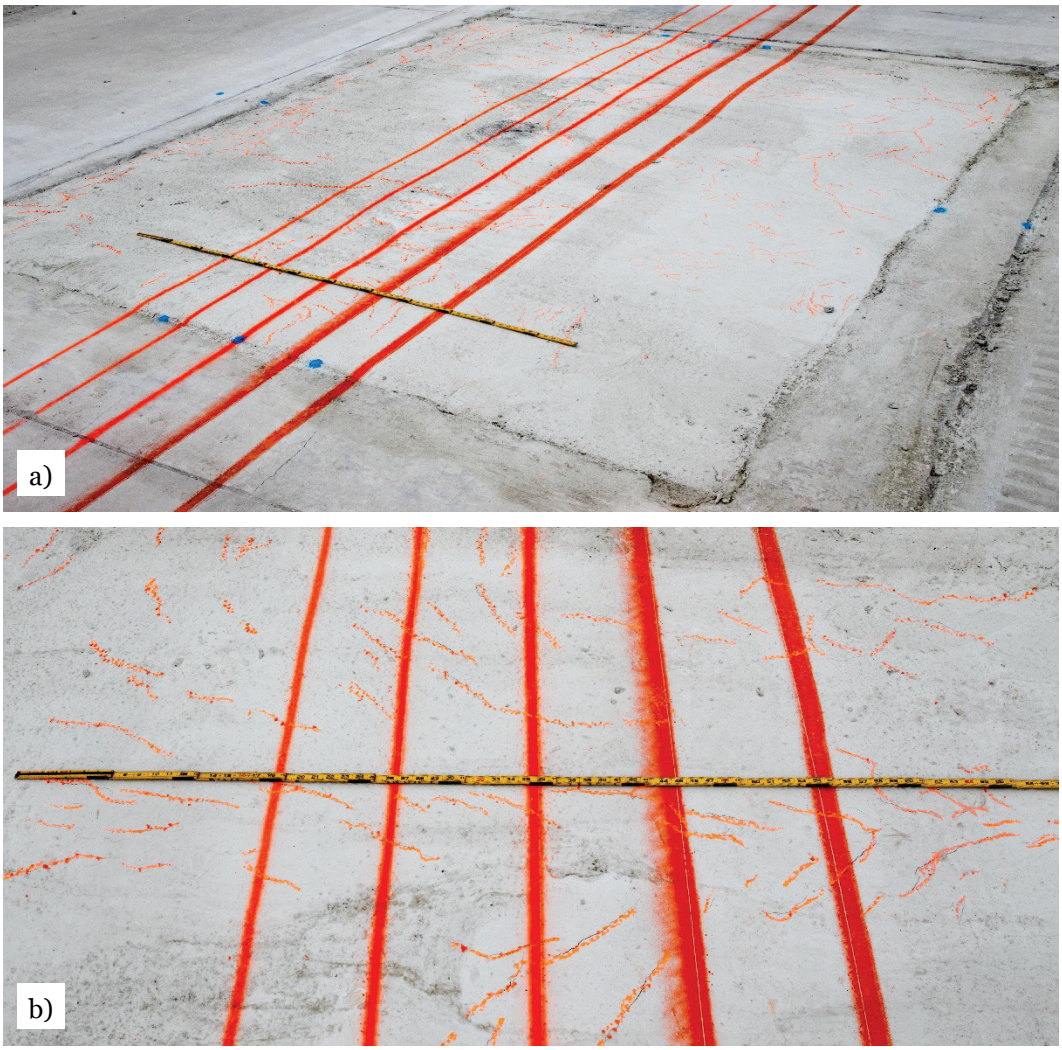


Figure 6.18. Medium-severity joint spall on foam backfill repair after 3,504 passes (Test #2).



Repair 2 was tested multiple times throughout trafficking by using the HWD to measure the stiffness of the pavement structure. The stiffness measurements showed a decrease with increasing passes. The stiffness data ranged from 1,347 kips/in. before traffic to 582 kips/in. after traffic. The survey data collected after 3,504 passes (876 coverages) showed a maximum elevation change of 0.60 in. This was observed at three locations along the south edge of the repair.

6.3 Test #3: Lighter and leaner RADR equipment; cement-stabilized silty sand backfill

6.3.1 Procedure

Test #3 used the lighter and leaner equipment set and cement-stabilized soil as the backfill material. Test #3 was conducted on 29 August 2017 with 10-mph winds, mostly cloudy skies, and air temperatures that increased from 75°F to 83°F. Light rain and a light thunderstorm began just after Repair 5 was capped. The wet weather did not affect the test.

The same lighter and leaner equipment and repair procedures described in Section 6.1.1 were used for this test. However, the large simplified volumetric mixer from the traditional RADR crater repair process was used for capping since the deployable mixer was inoperable. The only major difference between this test and Tests #1 and #2 was the backfill material and placement method used. The cement-stabilized silty sand was placed 12 in. thick for this backfill method.

During the initial debris removal process, the warehouse team strategically placed the backfill material close to the repair areas. The warehouse team staged 42 bags (92 lb each) of PLC using the Caterpillar TL642C telehandler. A tarp was placed over the PLC bags to prevent them from getting wet, since there was a threat of rain during the test.

Meanwhile, during the saw-cutting and excavation tasks, the backfill team blended the backfill soil. A diagram of the layout is provided in Figure 6.19 to show the staging of the blend areas to the crater repairs and stockpile. The volume of the silty-sand stockpile was estimated to be double the volume required for backfill to account for compaction and waste. The initial moisture content of the soil was measured at 6.6%, so additional water was added using the water truck (Figure 6.20) prior to blending to make sure the mix was wet enough for compaction. Typically, the optimum moisture content for silty sand used for cement-stabilized testing at ERDC has been 8%. The backfill team used the front-end loader to bring the backfill supplies, including two jumping jacks (Multiquip Mikasa MTX-70 rammers), two shovels, two rakes, and spray paint to the repair site.

Figure 6.19. Soil blending layout.

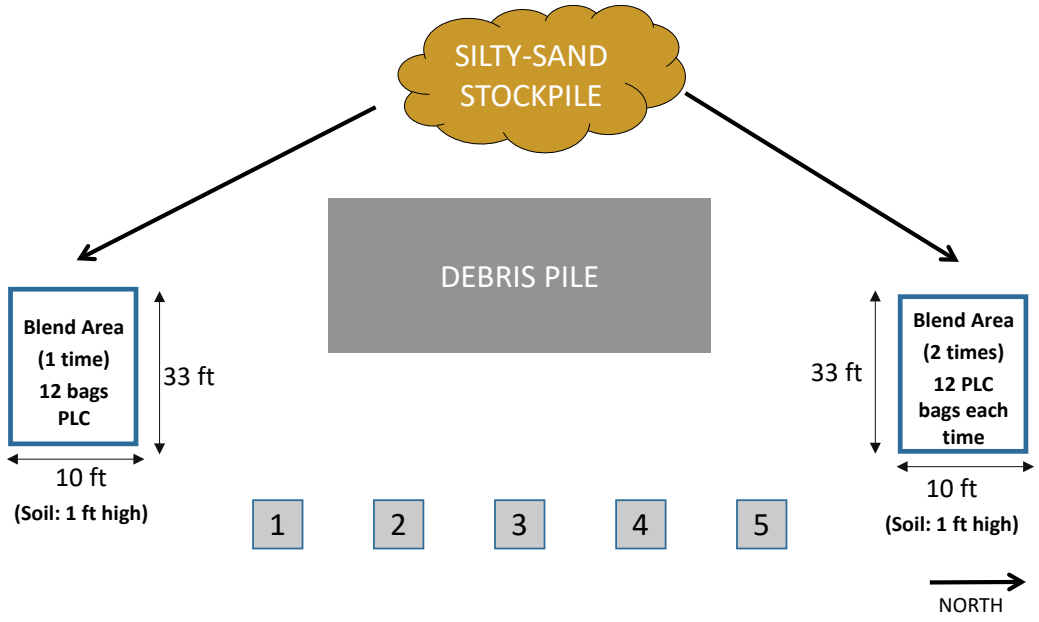


Figure 6.20. Addition of water to the silty sand stockpile in Test #3.



The soil-blending process is summarized in Figure 6.21. It started with marking a blend area that was 10 ft by 33 ft, which is faintly visible as a green painted line underneath the front-end loader in Figure 6.21a. The backfill team laid out the silty-sand soil approximately 1 ft high with the front-end loader and distributed 12 bags (92 lb each) of cement on top of the soil evenly in the blend area. This layout was completed to obtain a 5% PLC by dry weight of soil blend, which required 3.34 lb of PLC per cubic foot of loose soil.

The tiller attachment (Caterpillar LT13B) on the CTL was used to mix the soil, as shown in Figure 6.21c. The front-end loader was used to flip the soil to ensure the soil on the bottom was incorporated with the cement (Figure 6.21d). The mixing process took approximately 15 min per 10-ft-by-33-ft blend area. Two batches, one on the south end and the other on the north end of the repair site, were mixed in the beginning to create a stockpile that was ready to be placed and compacted once the excavation task was completed. Soil was mixed at the south blend site first, and the north blend site was used for both of the two subsequent mixing operations. The third and last batch, on the north end, was mixed after the backfill process had started for Repair 2.

Figure 6.21. Overview of soil-blending process in Test #3.



The backfill placement and compaction process is summarized in Figure 6.22. It consisted of placing the cement-stabilized soil in three 4-in.-thick compacted lifts to obtain a total thickness of 12 in. Lines were spray-painted on each wall of the excavated repairs to delineate the layers (Figure 6.22a). Soil was placed by the backfill team by using the front-end loader, shovels, and rakes (Figure 6.22b and Figure 6.22c). Each soil lift was placed 2 to 3 in. more than the desired level to account for compaction. The first two lifts were compacted with two passes of the jumping jack and four passes for the final lift (Figure 6.22d). The cement-stabilized backfill team included the front-end loader operator, the CTL with tiller operator, and two helpers. When the saw team of six airmen finished the last repair, they moved to Repair 3 to assist the backfill team, thereby augmenting the backfill team to a total of 10 airmen.

Figure 6.22. Overview of cement-stabilized backfill process in Test #3.



The cement-stabilized soil backfill process enabled the backfill team to work two repairs at a time because of the multiple lifts of soil required. When a lift of soil was added to one repair, a helper would use the jumping jack to compact the soil, and the front-end loader operator would retrieve more of the soil blend for a lift in the next repair. The compaction and addition of soil processes would alternate for each repair until all three lifts were complete. For the first two crater repairs, the backfill team compacted with the jumping jack for more than two passes because the silty sand had lost some moisture; it was difficult to determine that compaction had occurred. At Repair 3, the crater team leader had the water truck lightly sprinkle the soil-cement blend, which made it easier for the airmen to achieve satisfactory compaction. For the last two repairs, Repairs 4 and 5, the JCB 3CX backhoe with bucket (removal task) operator finished excavating the PCC and debris from the last repair and began assisting with adding the cement-soil mixture to the excavated repairs.

The capping process for each repair began approximately 10 to 30 min after the completion of backfill. The 30-min wait time before capping was implemented to allow more than one repair to be ready for capping to limit the amount of time spent washing out the volumetric mixer. Repairs

1, 2, and 3 were capped successively, then the mixer left the repair site for almost 20 min to be washed out.

During the screeding process of Repair 1, the ASTH got caught on the far edge of the repair as the telehandler boom was extending. Because the operator maintained a downward force on the ASTH and continued screeding, the sacrificial Nylatron® trim piece was sheared off the bottom of the screed bar, identifying an area needing improved robustness on the ASTH. This was beyond quick repair; therefore, the magnesium straight-edge bar and Wyco Screed King were used to screed the surface of the remaining repairs.

The final debris removal process did not include the FOD Boss. The FOD Boss did not perform well in Tests #1 and #2. It was also raining at the conclusion of the repairs, so the concrete dust at the repair site was wet. The final debris removal task was completed in the rain with two Ditch Witch SK850 mini skid steers.

After the repairs were capped, data collection, to include surveying, HWD testing (Figure 6.8), and visual inspection, was conducted in the rain. All capped repairs were trafficked 2 hr after the capping of Repair 5 with 112 passes (28 coverages) of the F-15E single-wheel load cart in a normally distributed wander pattern. The repair with the most noticeable damage, Repair 5, was trafficked further until 3,504 passes (876 coverages) or failure was achieved. Failure for this experiment was defined as a repair posing as a tire hazard, a high-severity shattered slab, or a slab containing a spall that was at minimum 24 in. long, 6 in. wide, and 2 in. deep. Periodic surface monitoring and HWD tests were conducted on Repair 5 during the trafficking process.

Post data collection was completed on Repair 5 after the completion of trafficking. This included surveying the surface to check for elevation changes, running HWD tests to estimate layer stiffness, extracting three cores from the repair to validate cap thickness, conducting two DCP tests on the cement-stabilized base via drilled holes to estimate the backfill material's CBR, and visually inspecting the repair surface for pavement distresses. The extracted cores were tested at ERDC to measure the Rapid Set Concrete Mix®'s 28-day ultra-compressive strength.

6.3.2 Results

The timed Test #3 started at 0740 and ended at 1206. The PCC parent slab dimensions and the crater repair timing results are shown in Table 6.5. The TTP times shown in Table 6.5 were developed with the traditional RADR crater repair equipment and with rapid-setting flowable fill as the backfill material; therefore, a comparison of the time difference between the two equipment sets and backfill methods was available. The TTP times shown are also for small crater repairs that are typically 8.5 ft by 8.5 ft (72 ft²). Repairs 2, 3, and 4 were closer in size to those described in the TTP, ranging from 65 ft² to 85 ft², while Repairs 1 and 5 were larger, with Repair 5 being more than double the area in the TTP.

Table 6.5. Repair characteristics and task times for Test #3 (lighter and leaner equipment and cement-stabilized silty sand backfill).

Repair			Time (min)						
No.	Area (ft²)	Parent Slab Thickness (in.)	Initial Debris Removal	Upheaval Marking	Saw-Cutting	Breaking	Excavation	Backfill	Capping
1	118[a]	8	2	3	15	5	29	49	22
2	85	8	4	2	20	7	24	56	17
3	65[a]	17	4	2	50	3	19	48	10
4	83	18	3	3	33	10	24	53	16
5	181	16	10	5	38	30	55	50	25
Average Time (min)			4.6	3	31.2	11	30.2	51.2	18
TTP	72	18	1.5	4.5	22	12	11	30	35

[a]Area was estimated because actual saw-cut lines were not completely visible.

The average upheaval marking, breaking, and capping times completed with the lighter and leaner equipment were comparable with the traditional RADR crater repair equipment, despite the larger repair sizes. The initial debris removal times for Repairs 2, 3, 4, and 5 appear skewed; however, these results were due to the technique the team used. The team made multiple parallel passes in a row, clearing parts of the debris from all four crater repairs with each pass. So, it essentially took a total of 10 min to clear the debris away from the five repair areas, which is approximately 2 min for each repair.

The average breaking time with the JCB backhoe hammer was comparable to the TTP breaking time of 12 min for a 72-ft² area, which uses the

traditional wheeled excavator. The backhoe operator took 30 min to break out the PCC crater damage on Repair 5. The excessive breakout time occurred because the operator was also spending time trying to move the larger broken pieces of PCC out of the damaged area with the backhoe hammer instead of allowing the removal team to remove the larger pieces. This action artificially increased the breaking time. The breaking process was not on the critical path; therefore, no tasks were waiting on the PCC breaking operator to get the job completed efficiently on Repair 5. Often times, the JCB backhoe used for breaking provided this minimal assistance to the JCB backhoe used for excavation. The times associated with excavating the PCC debris and soil using the JCB backhoe were generally slower than the goal written in the TTP when using the traditional wheeled excavator included in the RADR equipment set.

Backfilling with the cement-stabilized silty sand was the slowest crater repair task for this test and also increased the overall repair time, since capping cannot begin until backfill is completed. The backfill process time was longer than necessary because the backfill team, with the exception of Repair 5, performed more compaction coverages on each lift of the cement-stabilized silty sand than recommended. Each lift required two coverages of the jumping jack until the top lift, which required four coverages. However, the Airmen compacted each lift with up to five coverages. Additionally, the backfill team was backfilling two repairs at a time, with the exception of Repair 5. The process appeared to become more efficient with each repair, since Repair 5 took approximately the same amount of time as the other repairs even though Repair 5 was more than double in size. This could also be attributed to the increase in manpower, since the saw team assisted with backfilling starting with Repair 3.

The saw-cutting process varied in duration due to the differences in the thickness of the parent slabs. Additionally, during Repair 3, a saw-cutting operator had to return to the area to cut around PCC that was damaged from the backhoe bucket during the removal task, adding time to the sawing process for this repair. The saw spotter did not correctly align the saw-cutting operator, so an additional cut was made. Repair 3 received six full-length cuts instead of the typical four.

The saw-cutting rate goal in the TTP is 1 ft/min. The saw-cutting rates for the four cuts associated with each crater repair are shown in Table 6.6. The rates for the SW360B wheel saws ranged from 0.92 ft/min to 3.18 ft/min,

depending on the thickness and apparent strength of the PCC (strength was not measured). Repair 2 had very fast cutting rates that averaged 2.67 ft/min because the parent slab was only 8 in. thick. The rate for the Cuts Inc. SS 4200 HF diamond-blade saw ranged from 0.78 ft/min to 2.25 ft/min in the 16-in.-to-18-in.-thick PCC. The parent slabs around the repairs appeared to have a lower strength. It was difficult to measure the saw-cut lines for Repairs 1 and 3 because the capping material covered the repair edges.

Table 6.6. Saw-cutting rates for Test #3.

Repair No.	Saw Type[a]	Cut Length (in.)	Cut Time (min)	Cut Rate (ft/min)
1 (8 in. thick)	DB	—[c]	6	—[c]
	WS	—[c]	4	—[c]
	DB	—[c]	8	—[c]
	WS	141.0	4	2.94
2 (8 in. thick)	WS	114.5	3	3.18
	WS	115.5	4	2.41
	WS	140.0	5	2.33
	WS	130.5	4	2.72
3 (17 in. thick)	DB	108.0	4	2.25
	WS	108.0	5	1.80
	WS	—[c]	5	—[c]
	DB/WS[b]	—[c]	4/4	—[c]
4 (18 in. thick)	WS	120.0	10	1.00
	WS	122.0	11	0.92
	WS	115.0	9	1.06
	WS	123.0	9	1.14
5 (16 in. thick)	DB	172.0	8	1.79
	DB	169.5	18	0.78
	DB	176.5	8	1.84
	WS	186.5	14	1.11

[a] WS = Caterpillar SW360B wheel saw; DB = Cuts Inc. SS 4200 HF diamond-blade saw

[b] Both saws used since an additional cut was required

[c] Accurate measurement not possible since cut lengths were covered with repair materials

A Gantt chart showing the duration of each crater repair task for the five repairs is shown in Figure 6.23. The Gantt chart provides a timeline overview of the entire experiment, including the wait times between each crater repair task. The entire test was completed in 266 min. The Gantt chart shows that the excavating, backfilling, and capping tasks occurred simultaneously at the different repairs. The excavation task overlapped with the breaking task because the breaking task operator used the bucket at the front of the backhoe to help remove some of the broken debris out of the repair area.

The backfill task overlapped since the team backfilled two repairs at a time due to the soil installation process requiring placement and compaction in lifts. There was a 30-min wait time after backfilling and before capping on Repair 1 because the capping team waited until the cement-stabilized backfill placement was nearly completed on Repair 3 so that the Repairs 1, 2, and 3 could be capped in succession. The capping task overlapped between repairs because the mixer moved on to the next repair while the screeding and/or hand work was being completed on the current repair. The simplified volumetric mixer was washed out after capping Repairs 3 and 4.

The surface of Repairs 1, 2, 3, and 4 exhibited shrinkage cracks soon after the caps were placed (highlighted in orange in Figure 6.24). This was likely due to the capping material being placed too wet. The surface of Repair 5 had very few cracks; the material during placement was on the drier side compared to the previous four repairs in this test. All of the repairs were trafficked with 112 passes (28 coverages) of the F-15E load cart 2 hr after Repair 5 was completed. Repair 5, which consisted of the entire parent slab, was then selected for further trafficking. The repair did not show any additional visible surface distresses until 3,504 passes (876 coverages), at which point a minor low-severity joint spall on the north transverse joint had formed, as shown in Figure 6.25. Overall, the repair performed well under the simulated F-15E traffic.

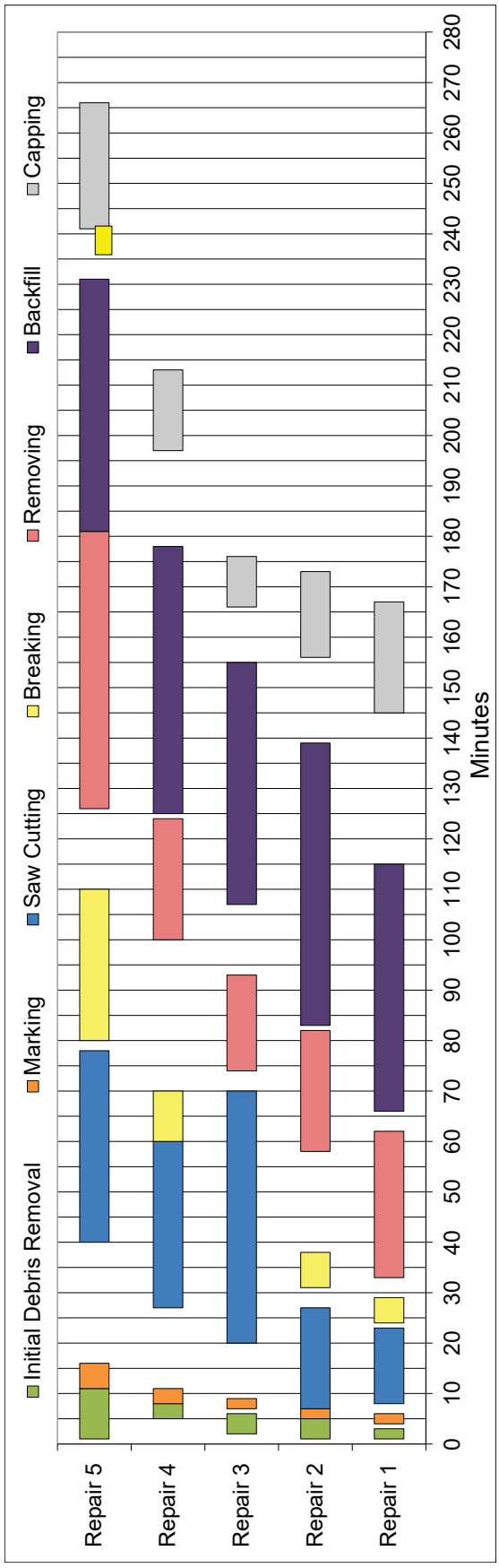


Figure 6.23. Gantt chart of overall progress with lighter and leaner crater repair equipment and cement-stabilized soil backfill (Test #3).

Figure 6.24. Typical shrinkage cracking on surface of cement-stabilized soil backfill repairs (Test #3).



Figure 6.25. Low-severity joint spall on cement-stabilized soil backfill repair at 3,504 passes (Test #3).



Repair 5 was tested multiple times throughout trafficking by using the HWD to measure the stiffness of the pavement structure. The HWD data showed that the impulse stiffness modulus (ISM) measurements stabilized after the initial placement. At 2 hr after capping, the ISM was 2,329 kips/in., and the ISM ranged from 3,100 kips/in. to 3,800 kips/in. during trafficking.

Repair 5 was surveyed for surface elevation changes before, during, and after trafficking. The data showed a maximum elevation change of 0.36 in. Repair 5 performed well under the F-15E traffic.

6.4 Test #4: Traditional equipment; geocells with sand backfill

6.4.1 Procedure

Test #4 consisted of performing five crater repairs with the traditional RADR crater repair equipment set and utilizing the geocell-reinforced sand backfill method. Aside from the backfill task, the traditional RADR crater repair process and equipment described in Chapter 4 were used. The weather during the test consisted of 14-mph winds, mostly cloudy skies, and air temperatures that increased from 80°F to 90°F.

The traditional RADR crater repair equipment set for the initial debris removal task consisted of one Caterpillar 926M front-end loader and one 289D XPS CTL with a bucket. Both machines worked continuously throughout the crater repair process to clean around the repair areas and push debris away from the repair area.

The marking team used the same tools and materials (stanchions, spray paint, and a metal beam) as the lighter and leaner RADR equipment set to mark the craters in the traditional manner. The marking team painted four lines outside of the pavement upheaval of each crater for the saw operators to follow.

The saw-cutting team used three Caterpillar 289D XPS skid steers and one Caterpillar 279D XPS skid steer. All were equipped with a Caterpillar SW360B wheel-saw attachment. Two wheel saws worked simultaneously beginning with Repair 1, while the other two wheel saws started cutting on Repair 2. The two saw spotters worked to clear the concrete sawdust from the marked lines with shovels and brooms during the cutting task. The saws continued cutting around the craters in sequence, where needed.

During the test preparation, the warehouse team began loading super sacks of Rapid Set Concrete Mix® from the warehouse tent and onto the tractor-trailer. After the completion of the saw-cutting task, the warehouse team began hauling the super sacks from the tractor-trailer to the repair areas using two telehandlers. The super sacks were staged strategically so that they were convenient for the capping task. Four warehouse team

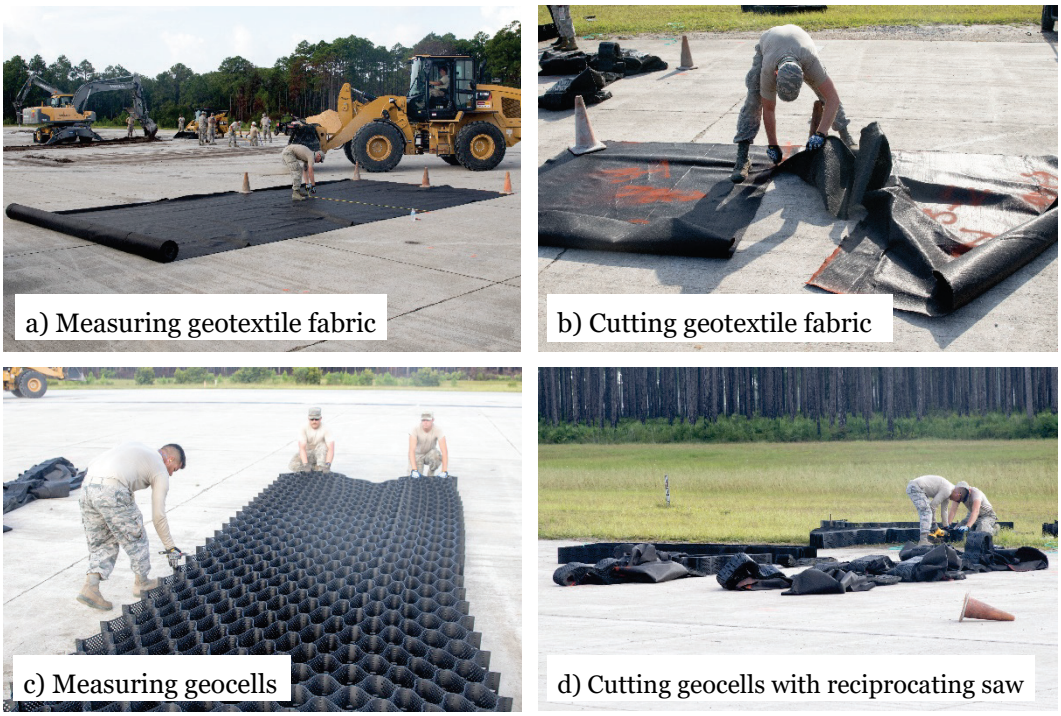
members were used to operate the tractor-trailer, two telehandlers, and the warehouse forklift.

The excavation task, which began as soon as saw-cutting on Repair 1 ended, was completed by using a Volvo EW180C wheeled excavator with a HB1400 moil-tipped hammer and a Volvo EW180C wheeled excavator with a toothed bucket. The moil-tipped hammer attachment broke the concrete inside the cut repair area into approximately 3-ft-size pieces or smaller, then the bucket removed the broken PCC and disturbed soil 26 in. deep from the top of the repairs. A spotter assisted the excavation team with the breaker and bucket placement and was responsible for keeping up with the depth of soil and PCC removal. The spotter also spray-painted small lines along the repair walls at 10 in. from the top of the repairs to indicate the required height of the backfill.

Once excavation was completed, the spotter and crater team leader finished the bottom of the excavated repair by leveling the surface with rakes and shovels and compacting with a Multiquip Mikasa MTX70 HD Rammer, or jumping jack. Since the saw-cutting team had completed their task on Repair 5 when the excavation was completed on Repair 2, three members of the saw-cutting team assisted with leveling the bottom of the excavation on Repairs 2, 3, 4, and 5.

While the initial debris removal, upheaval marking, saw-cutting, and excavation teams were completing their tasks, the backfill team was preparing the geocells on the edge of the runway (Figure 6.26). The backfill team's equipment set included the Caterpillar 279C XPS CTL with a bucket attachment, a Caterpillar 926M front-end loader, and a UTV. The Caterpillar 926M front-end loader was used to carry the geocell sections; nonwoven, 6-oz geotextile fabric; and the Northern Industrial JPC-80 Plate Compactor. The UTV was used to carry team members and tools -- such as utility knives, a reciprocating saw, a measuring tape, and rebar -- for cutting the geocell sections to the appropriate size. Hammers, backfill rakes, and shovels were also in the tool set to assist with preparation of the backfill in the repair. The Caterpillar 279C XPS CTL with the bucket attachment was later used to transport sand from the pile and into the repairs. As soon as the saw-cutting team finished cutting all edges of a repair, the crater team leader relayed the crater dimensions to the backfill team so that the geocell sections could be cut to size.

Figure 6.26. Measuring and cutting geotextile fabric and geocell sections in Test #4.



Backfilling with the geocells and sand consisted of using the Caterpillar 926M front-end loader to carry the precut geocells and fabric from the edge of the runway to each repair and using the Caterpillar 279C XPS CTL with a bucket attachment to transport sand from the sand pile and into the repairs. The front-end loader assisted with transporting sand from the pile to Repair 5, since all geocell sections had been removed from the bucket at that point. The installation of the geocell-reinforced sand backfill for each repair (Figure 6.27) was as follows.

1. The bottom of the excavation was lined with the 6-oz needle-punched nonwoven polypropylene geotextile fabric.
2. The first layer of geocells was expanded parallel to the centerline. Rebar was placed at all corners of the repair to hold the expanded geocell section in place. Sand was used to backfill some of the geocell pockets along the edges to help hold the geocell section in place.
3. The geocell section was backfilled by dropping sand vertically into the repair to avoid displacing the geocell section. The geocell section was overfilled by approximately 2 in.
4. The first layer was compacted using the Northern Industrial JPC-80 Plate Compactor until the sand appeared to be nearly level with the geocell section. Any excess material was struck off level with the top of the geocell by using shovels and rakes.

5. The surface of the first layer of geocells was then covered with the 6-oz nonwoven needle-punched polypropylene geotextile fabric.
6. The second layer of geocells was expanded perpendicular to the centerline and held in place, as described in Step 2.
7. The second layer of geocells was backfilled and compacted, as described in Steps 3 and 4.

The training sequence conducted previously showed that the installation of geocells and sand backfill appeared to be the most time-consuming task during the repair process. Therefore, members of the upheaval-marking, saw-cutting, and excavation teams assisted with the geocell-reinforced sand backfill installation once they had completed their tasks on all repairs. This allowed for the repair of three craters to occur simultaneously. For example, compaction of geocell layer 2 in Repair 1 occurred at the same time as compaction of geocell layer 1 in Repair 2 and installation and backfill of geocell layer 1 in Repair 3. At one point, 12 Airmen were working on the backfill task.

The final task in the timed crater repair process was to cap each repair with 10 in. of Rapid Set Concrete Mix®, as described in Chapter 4. The capping team included a military vehicle driver for pulling the large simplified volumetric mixer, a volumetric mixer operator, a water truck operator, an operator for the extendable boom forklift for keeping the mixer loaded with capping material, and two helpers to move the rapid-setting material around the repair with shovels. Two team members, the water truck operator and a helper, were from the marking team. They joined the capping team after the upheaval marking team's duties were finished. The capping process in Repair 1 began as soon as the backfill task was completed. For Repairs 2, 3, 4 and 5, the time between completion of the backfill task and the capping task ranged from 5 min to 50 min. The capping team capped two consecutive repairs before washing out the mixer, when time allowed. Each repair was finished by using the magnesium straight-edge bar or Wyco Screed King vibratory screed, depending upon the repair size.

Figure 6.27. Overview of geocell backfill installation process in Test #4.



Final debris removal was completed with the same personnel as the initial debris removal. This task was not timed because it was completed while waiting the 2 hr for the Rapid Set Concrete Mix® caps to cure. The equipment used for the final debris removal task included two Caterpillar 289D XPS CTLs with broom attachments.

After the repairs were capped, data collection -- including surveying, HWD testing, and visual inspection -- was conducted. Repair 5 was the only repair trafficked 2 hr after capping with 112 passes (28 coverages) of the F-15E single-wheel load cart in a normally distributed wander pattern. The repair was later trafficked further until 3,504 passes (876 coverages) or failure was achieved. Repairs 1, 2, 3, and 4 were not trafficked to minimize damage to the thin parent slabs between the repairs. Failure for this experiment was defined as a repair posing as a tire hazard, a high-severity shattered slab, or a slab containing a spall that was minimally 24 in. long, 6 in. wide, and 2 in. deep.

Data collection was completed on Repair 5 after trafficking. This included surveying the surface to check for elevation changes, running HWD tests to estimate layer stiffness, extracting three cores from the repair to validate cap thickness, conducting two DCP tests on the geocell-reinforced sand backfill via the cored holes to estimate the backfill material's CBR, and visually inspecting the repair surface for pavement distresses. The extracted cores were tested at ERDC to measure the Rapid Set Concrete Mix®'s 28-day ultimate compressive strength.

6.4.2 Results

The timed five-crater repair event of Test #4 started at 0755 and ended at 1130, for a total time of 3 hr 35 min. The three-crater repair training sequence with the lighter and leaner equipment set and geocell backfill was 3 hr 47 min. The training crater repairs took longer because of the smaller, less powerful equipment and since it was the Airmen's first attempt at repairing craters in sequence. The equipment operation and understanding of the crater repair sequence improved after each test.

The PCC parent slab characteristics and the crater repair timing results are shown in Table 6.7. The TTP times shown in Table 6.7 were developed with the traditional crater repair equipment and with flowable fill as the backfill material; therefore, a comparison of the time difference between the two backfill types was available. The TTP times shown are also for small crater repairs that are typically 8.5 ft by 8.5 ft (72 ft^2) and 18 in. thick. The repairs in this sequence ranged in size from 48 ft^2 to 107 ft^2 and were less than 18 in. thick.

Table 6.7. Repair characteristics and task times for Test #4 (traditional equipment and geocell-reinforced sand backfill).

Repair			Time (min)						
No.	Area (ft^2)	Parent Slab Thickness (in.)	Initial Debris Removal	Upheaval Marking	Saw-Cutting	Breaking	Excavation	Backfill	Capping
1	70	8	4	1	11	4	23	51	19
2	65	8	4	1	14	7	21	46	15
3	48	8	6	1	10	6	25	57	10
4	107	10	8	1	24	20	37	76	15
5	107	10	10	1	11	10	34	64	15
Average Time			6.4	1	14	9.4	28	58.8	14.8
TTP	72	18	1.5	4.5	22	12	11	30	35

Five of the seven crater repair tasks met the required times in the TTP. As with the previous tests, the initial debris removal team cleared the debris by making a single pass across one area of each repair rather than clearing one repair area at a time. The breaking task was longer than necessary for Repairs 2, 3, 4, and 5 because the operator spent much of the breaking time trying to flip or move the larger, broken PCC pieces out of the repair with the hammer. The excavation and backfill tasks were the slowest in the crater repair process for this test and did not meet the times in the TTP. Removal was slower because additional preparation was required at the bottom of the crater to properly install the geocells on a level surface. This additional prep work task is not required for backfills such as the flowable fill and foam. Even with the increase in manpower, the geocell-reinforced sand backfill took nearly twice as long as the flowable fill, mostly because the task requires considerably more steps and manual labor.

The saw-cutting rate goal in the TTP is 1 ft/min. The saw-cutting rates for the four cuts associated with each crater repair are shown in Table 6.8. The rates for the SW360B wheel saws ranged from 1.23 ft/min to 4.04 ft/min. The rate of 4.04 ft/min is uncharacteristically fast for a wheel saw, even in the thin PCC. Saw-cutting rates were considerably faster than required in the TTP, likely due to the thinner PCC slabs. The average saw-cutting time was nearly half the target time in the TTP.

Table 6.8. Saw-cutting rates for Test #4.

Repair No.	Saw Type[a]	Cut Length (in.)	Cut Time (min)	Cut Rate (ft/min)
1 (8 in. thick)	WS	101	3	3.22
		97.5	6	1.48
		99	3	3.18
		104.5	3	3.24
2 (8 in. thick)		100.5	4	2.43
		107.5	5	2.06
		90.5	4	2.13
		90.5	4	2.14
3 (8 in. thick)		75	4	1.86
		80	5	1.70
		87.5	3	2.78
		89.5	2	4.04
4 (10 in. thick)		120	9	1.27
		109	6	1.78
		134	6	1.99
		134	10	1.23
5 (10 in. thick)		121.5	5	2.36
		127	5	2.28
		123	4	2.88
		124	4	2.89

[a] WS = Caterpillar SW360B wheel saw

A Gantt chart for Test #4 repairs is shown in Figure 6.28. The Gantt chart provides a timeline overview of the entire experiment, including the wait times between each crater repair task. The saw-cutting and breaking tasks for Repair 4 overlapped. For this repair, the breaking process started at the opposite corner of a repair that was still being saw-cut by one saw. Also, the overlap between some of the crater repair tasks (excavation, backfill, and capping) can be viewed in the Gantt chart. The overlap between repairs with the excavation task was due to the breaking operator using the backhoe hammer to flip or move broken pieces of PCC out of the repairs. For backfilling, the team performed work on at least two repairs at a time and did not start backfilling Repair 1 until the excavation of Repair 2 was nearly completed. Also, Repairs 1 and 2 were capped consecutively, and the mixer was washed out after capping Repair 2. Repairs 3, 4, and 5 were also capped consecutively.

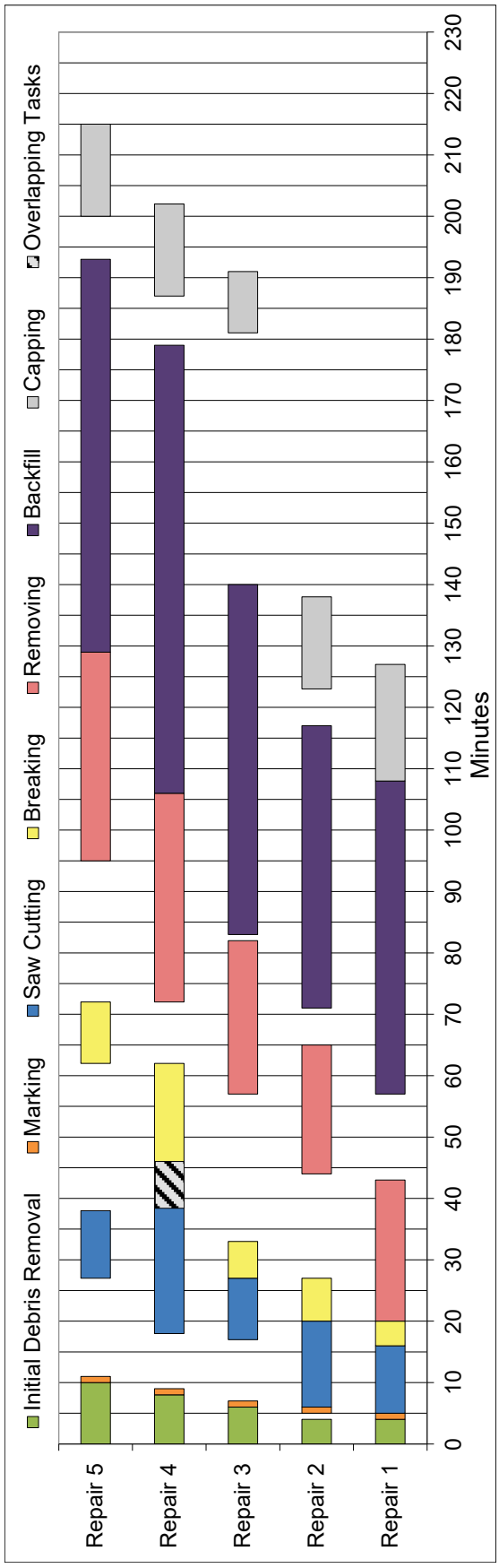


Figure 6.28. Gantt chart of overall progress with traditional crater equipment and geocells with sand backfill (Test #4).

The surface of Repair 5 exhibited shrinkage cracks soon after the caps were placed. This was likely due to the capping material being placed too wet at the surface. It was initially trafficked with 112 passes (28 coverages) of the F-15E load cart 2 hr after capping, and the condition remained the same until 1,056 passes (264 coverages) were applied. Medium-severity joint spalling on the south joint (Figure 6.29) and low-severity linear cracking on the centerline and east side (Figure 6.30) were noted. The condition remained relatively unchanged when trafficking was concluded after 3,504 passes (876 coverages). Overall, the repair performed well under the simulated F-15E traffic.

Repair 5 was tested multiple times throughout trafficking by using the HWD to measure the stiffness of the pavement structure. The stiffness measurements did not follow a trend with increasing passes. The stiffness data ranged from 800 kips/in. to 2,400 kips/in., which were lower than the flowable fill and cement-stabilized backfilled repairs.

Repair 5 was surveyed for surface elevation changes before, during, and after trafficking. The data showed a maximum elevation change of 0.36 in. at two locations in the centerline of the repair and at one location from the repair's cross section. Overall, Repair 5 showed good performance with the simulated F-15 traffic.

Figure 6.29. Medium-severity joint spalling on geocell backfill Repair 5 (Test #4).



Figure 6.30. Low-severity linear cracking on geocell backfill Repair 5 (Test #4).



6.5 Summary of test results

One of the most important aspects of crater repair is efficiency. Table 6.9 presents a comparison of the timing summary of the four tests from this experiment and two previous full-scale, troop-supported, small crater repair tests. It is difficult to directly compare the timing of the previous and current crater repair tests due to the variation of the crater repair sizes and wait times. The majority of the repairs using the lighter and leaner equipment set were larger than the crater repairs from the previous full-scale demonstrations.

Table 6.9 shows that the crater repair times using the lighter and leaner equipment set and the nontraditional backfill materials were within the timeframe of the crater repair tests conducted by using the traditional crater repair equipment set and flowable fill backfill, despite the larger repair sizes. The parent slab thicknesses of all repairs shown in Table 6.9 varied from 8 in. to 18 in., which typically affected saw-cutting, breaking, and excavation times.

Table 6.9. Timing summary of lighter and leaner experiment and previous crater repair demonstrations.

Test No.	No. of Repairs	Repair Team Size	Avg. Repair Size (ft^2)	Backfill Material	Target Backfill Thickness (in.)	Target Rapid Set Cap Thickness (in.)	Equipment Set	Repair Time
1	5	29	127	Flowable Fill	14	10	Lighter and Leaner	4 hr 2 min[a]
2	5	29	91	Polyurethane Foam	14	10	Lighter and Leaner	4 hr 47 min
3	5	29	106	Cement-Stabilized Silty Sand	12	10	Lighter and Leaner	4 hr 26 min
4	5	28	79	Sand-Filled Geocells	16	10	Traditional	3 hr 35 min
n/a	5	23	63	Flowable Fill	22	9	Traditional	4 hr 40 min[b]
n/a	6	25	72	Flowable Fill	24	10	Traditional	3 hr 44 min[c]

[a] Only two repairs were capped

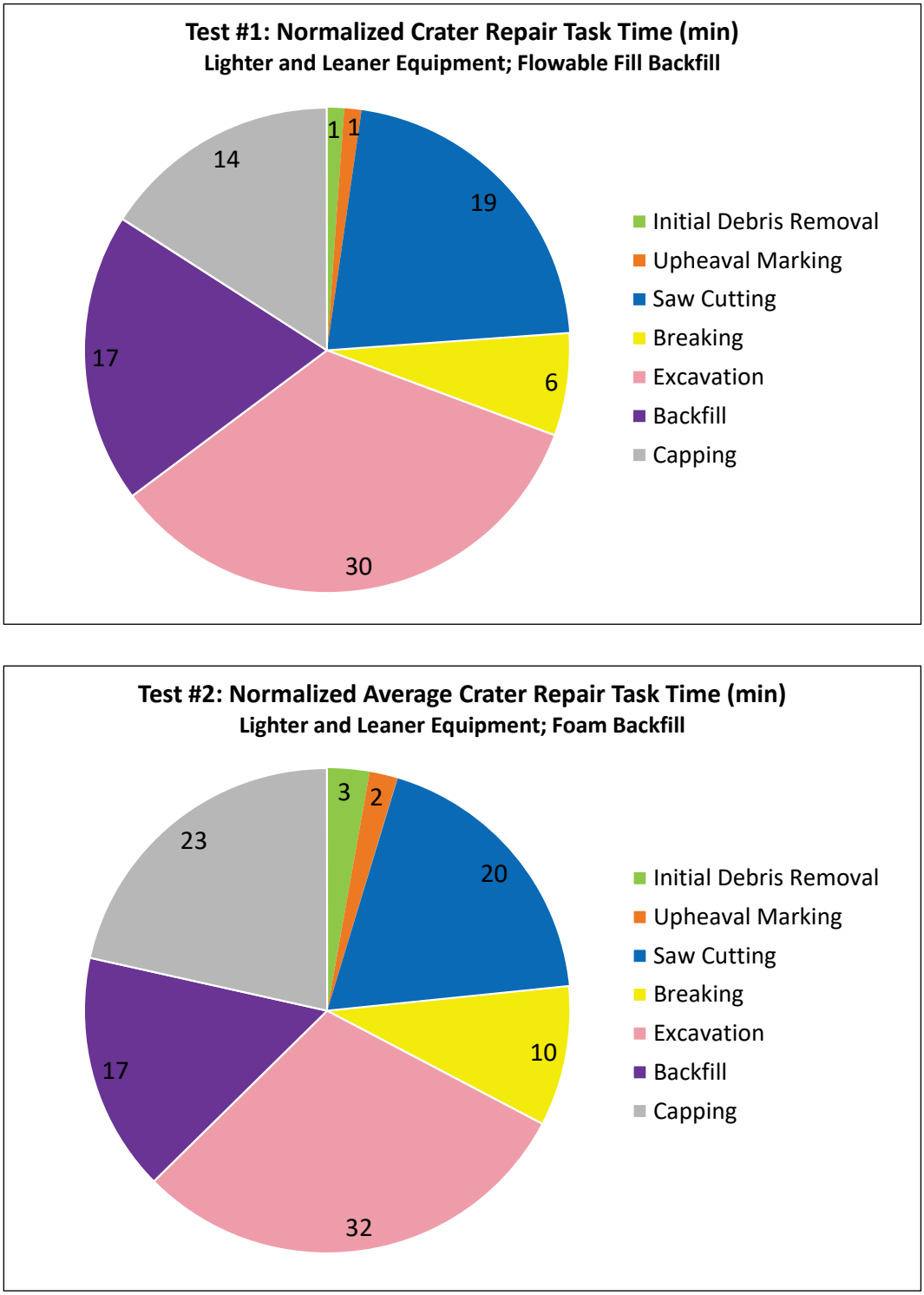
[b] Edwards et al. 2013

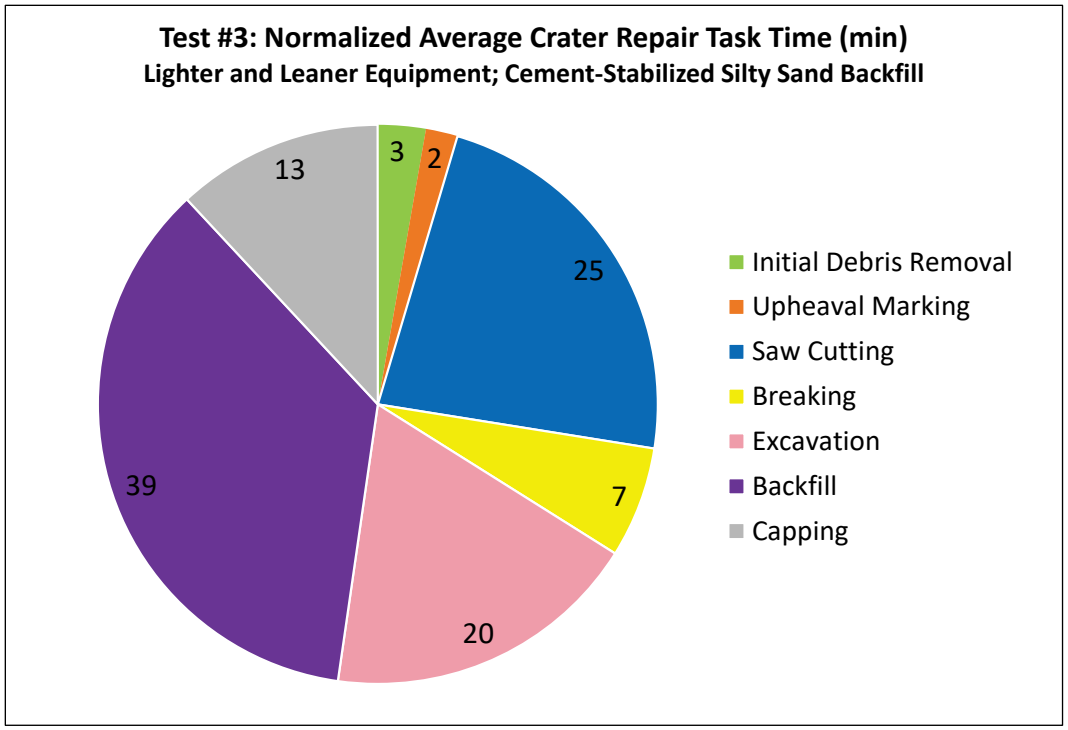
[c] Bell et al. 2013

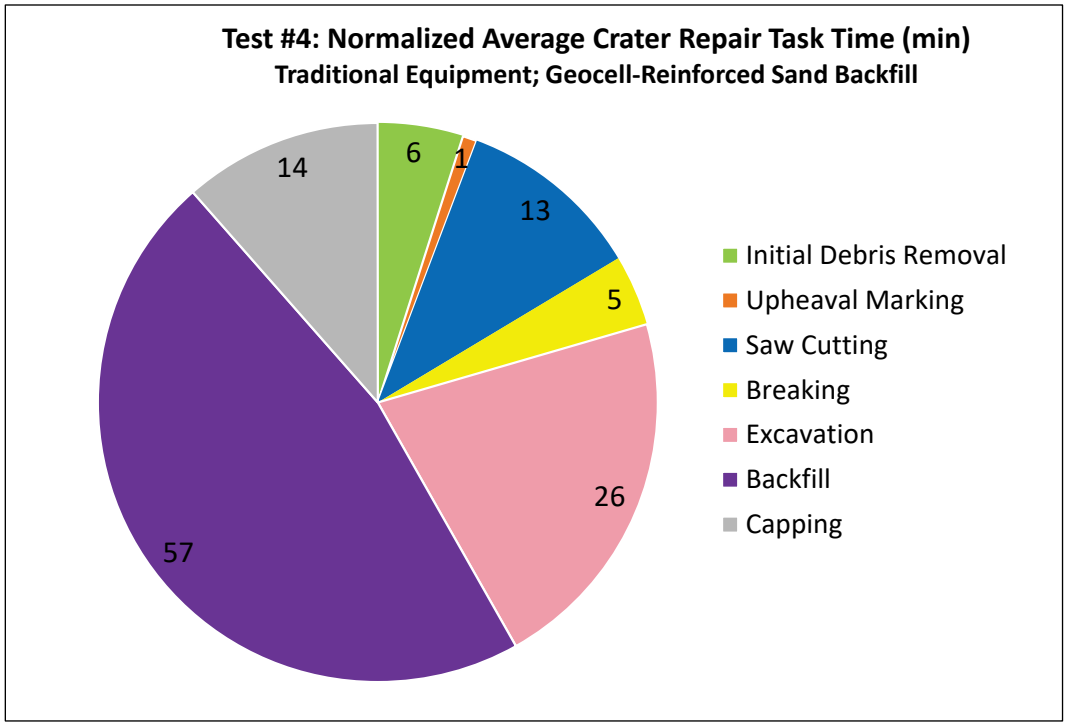
The test using the lighter and leaner equipment set with flowable fill as the backfill material (Test #1) likely would have been approximately 1.5 to 2 hr longer than the 4 hr 2 min time if the mixer had remained operable and the remaining three repairs had been capped. The lengthy crater repair time of Test #1 was likely due to the inexperience of the Airmen as equipment operators and due to this being the first of four tests. The operators improved their efficiency with each test.

For direct comparison purposes, Figure 6.31 presents a timing summary of the four tests from this experiment normalized using a repair area of 72 ft^2, which is the size of a typical small crater (8.5 ft by 8.5 ft). Normalizing the data to an area of 72 ft^2 makes it easier to compare the average timing results among the tests due to the variation of the repair sizes. The data shown in Figure 6.31 is the average time per crater repair task for each test and does not include any wait times between the repair tasks, which were displayed in the Gantt charts presented earlier.

Figure 6.31. Normalized average crater repair task timing summary for each test.







Each of the four tests experienced a weak link or a task that was much slower than the others, causing other crater repair task teams to wait. During Test #1 with the lighter and leaner equipment and flowable fill as backfill, excavating with the backhoe was the slowest task in the repair

process. This was also the case for Test #2. Typically, when using the traditional crater repair equipment set with flowable fill backfill, saw-cutting is the slowest task in the crater repair process. Test #3, which included backfilling with cement-stabilized soil, showed that backfilling was the weak link for efficiency purposes. However, the airmen excessively compacted the cement-stabilized soil backfill, unnecessarily increasing the average backfill time by approximately 10 min. Backfilling with the sand-filled geocells was the slowest task for Test #4, which used the traditional repair equipment. Backfilling in Tests #3 and #4 also employed ten Airmen (saw-cutting team assisted), while the other backfill teams for flowable fill and foam employed four or five Airmen. The decision was made after training with geocells and cement-stabilized soil that those backfill teams needed more manpower.

The excavation from Test #4 was used with the larger wheeled excavator. The excavation from Test #4 was essentially the same time as the excavations from Tests #1, #2, and #3 using the backhoe. This indicates excavation is not necessarily dependent on equipment size and power. Operator experience can also have a large influence on the excavation efficiency. The excavation and backfill tasks were responsible for approximately 50 to 80% of the crater repair time for the tests. Furthermore, capping the repairs by using the smaller deployable mixer was as efficient as capping the repairs by using the larger volumetric mixer.

Saw-cutting was responsible for approximately 10 to 23% of the time for the test sequences, depending upon the PCC thickness. The average PCC thickness in Test #4 was 9 in., which is why only 10% of the time spent repairing the crater was saw-cutting. The average PCC thickness for Tests #1, #2, and #3 was approximately 13 in., resulting in 20 to 23% of the repair time needed for saw-cutting.

Table 6.10 provides a comparison summary of the backfill placement task for each of the four tests. Backfilling with dry-placed flowable fill using the traditional crater repair equipment has, on average, ranged from 15 min to 30 min when conducted by using troop support at previous demonstrations (Edwards et al. 2013, Bell et al. 2013, and Pullen et al. 2014). The backfill task from the previous demonstrations were also performed in 8.5-ft by 8.5-ft (72 ft^2) repairs. The repairs from the RADR experiment were typically larger.

Table 6.10. RADR experiment backfill task summary.

Test No.	Backfill Material	Normalized Average Placement Time (min)	Manpower	Equipment Set
1	Dry-Placed Flowable Fill	17	4	Lighter and Leaner
2	Polyurethane Foam	17	4	Lighter and Leaner
3	Cement-Stabilized Silty Sand	39	4 – 10	Lighter and Leaner
4	Geocells with Sand	57	4 – 10	Traditional
TTP	Dry-Placed Flowable Fill	30	4	Traditional

Table 6.10 shows that polyurethane foam placement is just as efficient as dry-placed flowable fill when normalizing the data to 72 ft^2. However, the foam is much more logistically friendly due to the foam's ability to expand to six times its original liquid volume. When backfilling with modified indigenous materials (i.e., cement-stabilized silty sand and geocell-reinforced sand), the required time and manpower needed is two to three times more than what is required of rapid-setting flowable fill or polyurethane foam backfills. The trade-off is that the economical and logistical benefits are improved with some increased time and manpower.

Table 6.11 shows the thickness and compressive strength results from the three cores extracted from each repair that was trafficked to 3,504 passes (876 coverages). The cores were removed from the center, north, and south locations of the trafficked repairs. The surface thickness target was 10 in.; however, the average thickness of each of the trafficked repairs ranged from 10.5 to 12.1 in. The 28-day compressive strength of the cores from Test #1 was 6,940 psi. This is consistent with data from previous crater repair tests (Bell et al. 2013; Edwards et al. 2013). However, compressive strengths obtained from Tests #2, #3, and #4 were much higher, with averages ranging from 9,470 to 10,110 psi. All repair PCC caps exceed 5,000 psi compressive strength, which is the typical compressive strength for airfield quality PCC.

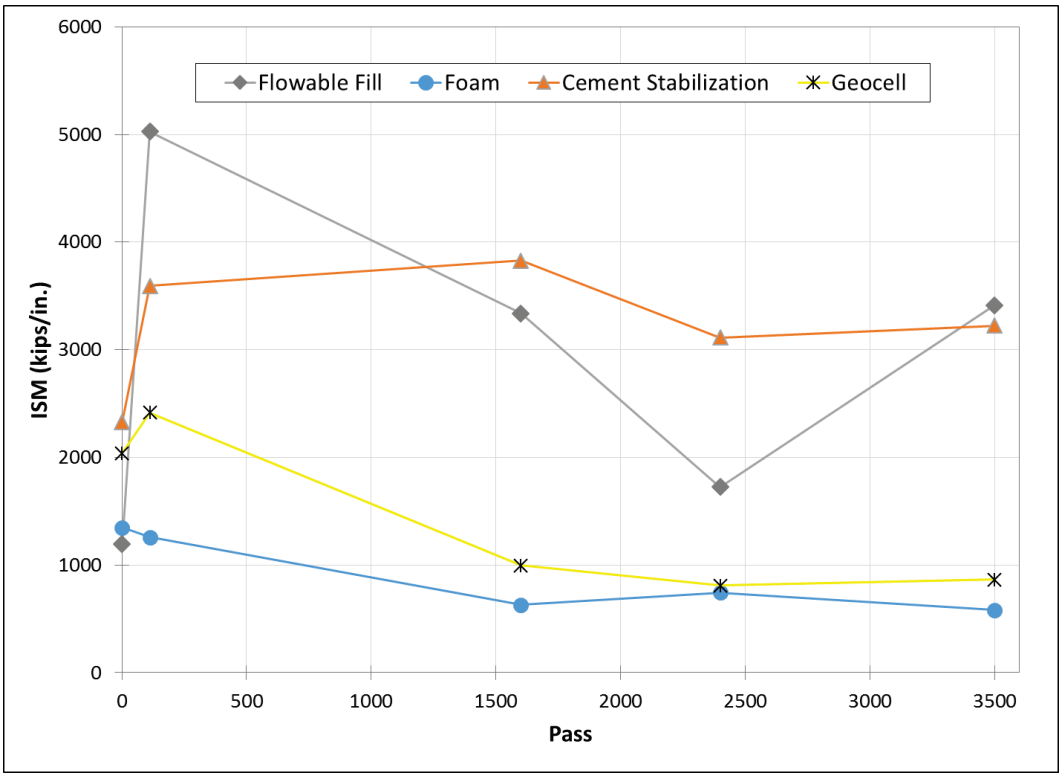
Table 6.11. Cored Rapid Set Concrete Mix® thickness and compressive strength data.

Test No.	Backfill Type	Average Cored Cap Thickness (in.)	Standard Deviation	Average 28-Day Compressive Strength (psi)	Standard Deviation
1	Flowable Fill	11.2	0.18	6,940	1,450
2	Foam	10.5	0.57	10,920	380
3	Cement-Stabilized Silty Sand	11.2	0.10	9,470	120
4	Geocells with Sand	12.1	0.28	10,110	100

HWD data was periodically measured from the center of each repair that was trafficked to 3,504 passes (876 coverages). Figure 6.32 shows the data measured from the tests. The HWD data show that the pavement structures from Test #1 (flowable fill backfill) and Test #3 (cement-stabilized silty sand backfill) had similar trends and were the stiffest compared to Test #2 (foam backfill) and Test #4 (geocells with sand backfill). This result was expected since flowable fill and cement-stabilized soil typically exhibit higher strengths than foam and geocell backfills due to the presence of cementitious materials.

Two DCP tests were conducted in drilled holes from a north and south location of the trafficked repair of each type of backfill material to estimate each material's CBR. Flowable fill and cement-stabilized silty sand DCP tests both resulted in refusals, which is an indication of a material with a CBR of 100. The average estimated CBR in the foam and geocells with sand was 9% and 4%, respectively. The DCP results are consistent with the HWD results, which showed that the pavement using foam and geocell-reinforced backfill were the weakest. A DCP test was also conducted on the soil material just off the PCC runway. The test results indicated the natural subgrade of the crater repairs had a CBR of 15.

Figure 6.32. HWD data of crater repairs with various backfill material.



All trafficked crater repairs achieved at least 112 passes (28 coverages) of the F-15E single-wheel load cart after 2 hr of cure time without any sign of impending failure. The repair from each test showing the most potential for failure was selected for further trafficking. Those repairs, which included the four different backfill types, were trafficked to 3,504 passes (876 coverages) and resulted in minimal surface distresses. The common surface distress noted from each trafficked repair was low-severity joint spalling. This confirms that all backfill types are suitable repair options for supporting aircraft traffic.

Logistics is another important aspect of crater repair, particularly because of the large amount of equipment and materials required. Table 6.12 presents a generic comparison of the weight and shipping volumes of the majority of the equipment required to complete the repairs by one crater repair team (18 small repairs). The weights and volumes shown were derived from the manufacturers' specifications. The equipment for the backfill task is shown for dry-placed flowable fill material.

Table 6.12. Generic RADR crater repair equipment weights and volumes for one crater repair team.

Crater Repair Task	Lighter and Leaner RADR			Traditional RADR		
	Equipment	Weight (lb)	Volume (ft^3)	Equipment	Weight (lb)	Volume (ft^3)
Debris Removal	Mini Skid Steer	3,100	145	Front-End Loader	28,770	3,371
	Mini Skid Steer	3,100	145	CTL	9,893	443
	Ride-On Sweeper	3,570	195	Broom	905	69
	Ride-On Sweeper	3,570	195	Broom	905	69
Sawing	CTL	9,893	443	CTL	9,893	443
	CTL	9,893	443	CTL	9,893	443
	CTL	9,893	443	CTL	9,893	443
	CTL	9,893	443	CTL	9,893	443
	Wheel Saw	3,420	275	Wheel Saw	3,420	275
	Wheel Saw	3,420	275	Wheel Saw	3,420	275
	Wheel Saw	3,420	275	Wheel Saw	3,420	275
	Diamond-Blade Saw	980	100	Wheel Saw	3,420	275
Breaking	Backhoe	17,527	1,868	Excavator	42,946	2,503
	Hammer	728		Hammer	2,932	
Excavation	Backhoe	17,196	2,035	Excavator	42,946	2,503
Backfill (dry flow fill)	Water Truck			Water Truck		
	Telehander	21,245	1,140	Telehander	34,361	1,426
Capping	Small Mixer	10,000[a]	1,944	Mixer	17,000[a]	1,872
	Water Truck			Water Truck		
	Telehandler	21,245	1,140	Telehandler	34,361	1,426
	Screed	1,000[a]	312			
	Telehandler	21,245	1,140			
Warehouse	Tractor/Trailer			Tractor/Trailer		
	Telehandler	21,245	1,140	Telehandler	34,361	1,426
	Telehandler	21,245	1,140	Telehandler	34,361	1,426
	Warehouse Forklift			Warehouse Forklift		
	TOTAL:	205,828	15,236	TOTAL:	319,993	19,407

[a] Estimated

When using the lighter and leaner RADR equipment set instead of the traditional RADR equipment set, the shipping weight and volume are decreased by approximately 114,165 lb and 4,170 ft^3, respectively, per crater repair team, or 799,155 lb and 29,190 ft^3, respectively, for seven crater repair teams. An estimated 36% decrease in shipping weight and an estimated 21% decrease in shipping volume occurs by using the lighter and leaner equipment instead of the traditional equipment.

7 Conclusions and Recommendations

For this project, ERDC assessed lighter and leaner RADR equipment, materials, and methods for performing small crater repairs. The ERDC team trained a group of 28 airmen in crater repair techniques using the traditional and the lighter and leaner crater repair equipment. The airmen were also trained by members of the ERDC team on backfill placement using flowable fill, geocells with sand, cement-stabilized silty sand, and polyurethane foam. Four full-scale field tests were then conducted by the airmen using a combination of the two types of equipment sets and the four backfill materials. The lighter and leaner technologies were compared with the traditional equipment set and materials for repairing small bomb craters. All repairs were capped with Rapid Set Concrete Mix®. The performances of the repairs were evaluated under simulated heavy military aircraft traffic. The following conclusions and recommendations were determined from the RADR technology integration experiment.

7.1 Conclusions

1. The lighter and leaner technology integration experiment resulted in successful and cost-effective crater repair solutions with some increases in repair time compared with using the traditional crater repair equipment and flowable fill backfill material.
2. The shipping volume and the weight of crater repair equipment for one 29-man crater repair team is decreased by an estimated 21% and 36%, respectively, when using the lighter and leaner equipment set.
3. All repairs were able to sustain the threshold of 112 passes (28 coverages) of the F-15E load cart after 2 hr of cure time. No additional surface distresses were observed after the initial 112 passes (28 coverages) when compared to the surfaces before trafficking.
4. The repair from each of the four test sequences selected for trafficking beyond 112 passes (28 coverages) sustained 3,504 passes (876 coverages) of the F-15E load cart with minimal cracking and spalling.
5. The FOD Boss used for the final debris removal task was not effective for collecting the large amount of concrete dust and debris associated with crater repairs.
6. The DitchWitch SK850 mini skid steers were effective at clearing debris from around craters as long as the thicker PCC pieces (greater than 15 in.) were not any wider than the 44-in.-wide bucket.

7. The Tennant S20 mid-size rider sweepers were effective at cleaning concrete dust and small aggregate from around the crater repairs during the final debris removal task.
8. After normalizing the timing data to one crater repair size, the results showed that the lighter and leaner JCB 4CX backhoe with a HM033T hydraulic breaker used for breaking the PCC was as efficient and effective as the traditional Volvo EW180C excavator with a HB1400 hydraulic breaker.
9. After normalizing the data to one crater repair size, the results showed that the lighter and leaner JCB 3CX backhoe used for excavating was as efficient and effective as the traditional Volvo EW180C excavator.
10. The deployable volumetric concrete mixer appeared to operate adequately; however, it is important to ensure it is constantly loaded due to the small bin size. The average timing results revealed that, after normalizing the timing data to one repair size area, capping with the deployable concrete mixer (14 min) was completed in approximately the same amount of time as capping with the larger volumetric mixer (13 to 23 min).
11. The Cuts Inc. SS 4200 HF diamond-blade saw was generally faster than the traditional Caterpillar SW360B wheel saw, particularly with PCC greater than 10 in. thick. With 8- to 10-in.-thick PCC, the wheel saw and diamond-blade saw had similar cut rates. The diamond-blade saw attachment cut at a faster rate than the wheel-saw attachments in PCC greater than 10 in. thick. There were no issues with excavating the broken PCC inside of repairs cut with the diamond-blade saw as long as the corners were cut full-depth and there was at least one cut made with a wheel saw. Furthermore, the diamond-blade saw was able to cut through steel dowels when the wheel saw could not cut through dowels.
12. The ASTH was faster than the traditional screeds and provided time for additional passes for screeding, if required. The ASTH also reduced the labor and manpower needed to perform the screeding process from three to six personnel to two personnel.
13. The repairs with the geocell-reinforced sand backfill performed well under simulated F-15E traffic and were a suitable alternative to flowable fill under the conditions of this experiment (10-in.-thick Rapid Set Concrete Mix® cap). Geocells continue to provide a small logistical footprint but require significantly more manpower (10 airmen) for installation than other backfill repair methods (4 airmen) described in this report. Also, the removal of broken PCC and soil is slower when backfilling with geocells since additional preparation is

required at the bottom of the excavation to properly install the geocells on a level subgrade surface.

14. Repairs with foam backfill performed well under simulated F-15E traffic and proved to be a suitable alternative to flowable fill when placed under a 10-in.-thick Rapid Set Concrete Mix® cap. After normalizing the timing data to one crater repair size, the results showed that backfilling with the foam was just as efficient as backfilling with rapid-setting flowable fill (average of 17 min per repair). However, the logistical footprint of the foam is decreased when compared to the flowable fill.
15. A layer of 12 in. of compacted silty sand mixed with 5% cement was comparable to flowable fill for 3,504 passes (876 coverages) of a simulated F-15E under a 10-in.-thick Rapid Set Concrete Mix® cap. The backfill placement time with the cement-stabilized soil is longer; however, the cement-soil mixture could be used when flowable fill is not available, possibly with locally available materials. Additional labor of 10 total airmen was required when placing the cement-stabilized soil backfill. After normalizing the timing data to one crater repair size, the results showed that backfilling with cement-stabilized soil was more efficient than backfilling with geocell-reinforced sand but not as efficient as backfilling with flowable fill or foam.
16. The backfilling task written in the TTP requires four team members. However, the experiment showed that more team members are needed when backfilling with geocells and cement-stabilized soil. These two tests utilized ten team members each. The additional six personnel were obtained from the saw-cutting team once the saw-cutting duties were completed.
17. The HWD data showed that the pavement structures from Test #1 (flowable fill backfill) and Test #3 (cement-stabilized silty sand backfill) had similar trends and were the stiffest compared to Test #2 (foam backfill) and Test #4 (geocells with sand backfill). The DCP results were also consistent with the HWD results, which showed that the backfill strengths of the repairs using foam and geocells were the weakest. However, all pavement structures provided sufficient bearing capacity to support over 3,500 F-15E passes.
18. The three core samples extracted from each repair trafficked to 3,504 passes (876 coverages) had average 28-day compressive strengths ranging from 6,940 psi to 10,920 psi. The strengths of the Rapid Set Concrete Mix® exceeded the 5,000-psi compressive strength requirements typically specified for PCC airfield pavements.

7.2 Recommendations

1. It is recommended to consider the implementation of the lighter and leaner equipment tested in this experiment for small crater repairs, with the exception of the FOD Boss. The small volumetric concrete mixer needs to be evaluated more using troop labor since it malfunctioned early in the experiment.
2. Flowable fill, polyurethane foam, cement-stabilized silty sand, or geocells with sand are recommended as backfill material options for small crater repairs.
3. For cement-stabilized silty sand, the moisture of the soil should be on the wet side with up to 10% moisture content. If sufficient moisture is not present, water can be added when compacting. The lack of adequate water content causes problems in achieving adequate compaction.

References

Air Force Civil Engineer Center. 2016. *Interim tactics, techniques, and procedures: Airfield damage repair (ADR) interim process for base recovery after attack*. Tyndall Air Force Base, FL: Air Force Civil Engineer Support Center.

ASTM International. 2007. Standard test method for particle-size analysis of soils. Designation: D422-63e2. West Conshohocken, PA: ASTM International.

_____. 2010. *Standard test methods for liquid limit, plastic limit, and plasticity index of soils*. Designation: D4318-10e1. West Conshohocken, PA: ASTM International.

_____. 2012. *Standard test methods for laboratory compaction characteristics of soil using modified effort (56,000 ft-lb$_f$/ft^3 (2,700 kN-m/m^3))*. Designation: D1557-12e1. West Conshohocken, PA: ASTM International.

_____. 2014a. *Standard practice for classification of soils for engineering purposes (Unified Soil Classification System)*. Designation: D2487-11. West Conshohocken, PA: ASTM International.

_____. 2014b. *Standard test methods for specific gravity of soil solids by water pycnometer*. Designation: D854-14. West Conshohocken, PA: ASTM International.

_____. 2018. Standard specification for blended hydraulic cements. Designation: C595/C595M-18. West Conshohocken, PA: ASTM International.

Bell, H. P., L. Edwards, W. D. Carruth, J. S. Tingle, and J. R. Griffin. 2013. *Wet weather crater repair testing at Silver Flag Exercise Site, Tyndall Air Force Base, Florida*. ERDC/GSL TR-13-42. Vicksburg, MS: U.S. Army Engineer Research and Development Center.

Bell, H. P. and J. Rowland. 2017. *Rapid airfield damage recovery: Deployable saw technology evaluation*. ERDC/GSL TR-17-29. Vicksburg, MS: U.S. Army Engineer Research and Development Center.

Bell, H. P. and J. S. Tingle. 2017. *Inclement weather crater repair tool kit*. ERDC/GSL TR-17-26. Vicksburg, MS: U.S. Army Engineer Research and Development Center.

Edwards, L., H. P. Bell, W. D. Carruth, J. R. Griffin, and J. S. Tingle. 2013. *Cold weather crater repair testing at Malmstrom Air Force Base, Montana*. ERDC/GSL TR-13-32. Vicksburg, MS: U.S. Army Engineer Research and Development Center.

Priddy, L. P., J. S. Tingle, M. C. Edwards, J. R. Griffin, and T. J. McCaffrey. 2013a. *Critical Runway AssessmenT and Repair (CRATR) technology demonstration: Limited operational utility assessment 2 (LOUA2), Tyndall Air Force Base, Florida*. ERDC/GSL TR-13-39. Vicksburg, MS: U.S. Army Engineer Research and Development Center.

Priddy, L. P., J. S. Tingle, J. R. Griffin, M. C. Edwards, and T. J. McCaffrey. 2013b. *Critical Runway AssessmenT and Repair (CRATR) technology demonstration: Operational utility assessment (OUA), Avon Park Air Force Range, Florida*. ERDC/GSL TR-13-33. Vicksburg, MS: U.S. Army Engineer Research and Development Center.

Pullen, A., C. Jackson, and B. Cotter. 2014. *2013 Wet weather HMA crater repair technology demonstration*. AFCEC-CX-TY-TR-2014-0026. Panama City, FL: Applied Research Associates.

Robinson, J., J. S. Tingle, and C. A. Rutland. 2016. *Material handling equipment evaluation for crater repair*. ERDC/GSL TR-16-30. Vicksburg, MS: U.S. Army Engineer Research and Development Center.

Robinson, J. H. and C. P. Rabalais. 1993. *Performance of the combat engineer vehicle with mineplow operating worldwide and in theaters of operations*. TR GL-93-23. Vicksburg, MS: U.S. Army Engineer Waterways Experiment Station.

Strange, R. C., J. S. Tingle, D. E. Yule, and C. A. Rutland. 2017. *Modernization of deployable airfield debris removal equipment*. ERDC/GSL TR-17-2. Vicksburg, MS: U.S. Army Engineer Research and Development Center.

Tingle, J. S., L. P. Priddy, C. Gartrell, M. Edwards, and T. J. McCaffrey. 2009. *Critical Runway AssessmenT and Repair (CRATR) limited operational utility assessment 1 (LOUA1), Tyndall Air Force Base, Florida*. ERDC/GSL TR-09-12. Vicksburg, MS: U.S. Army Engineer Research and Development Center.

United States Air Force. 1992. *Crushed-stone crater repair and line-of-sight profile measurement for rapid runway repair*. T.O. 35E2-5-1. Washington, DC: U.S. Air Force.

REPORT DOCUMENTATION PAGE

Form Approved
OMB No. 0704-0188

Public reporting burden for this collection of information is estimated to average 1 hour per response, including the time for reviewing instructions, searching existing data sources, gathering and maintaining the data needed, and completing and reviewing this collection of information. Send comments regarding this burden estimate or any other aspect of this collection of information, including suggestions for reducing this burden to Department of Defense, Washington Headquarters Services, Directorate for Information Operations and Reports (0704-0188), 1215 Jefferson Davis Highway, Suite 1204, Arlington, VA 22202-4302. Respondents should be aware that notwithstanding any other provision of law, no person shall be subject to any penalty for failing to comply with a collection of information if it does not display a currently valid OMB control number. **PLEASE DO NOT RETURN YOUR FORM TO THE ABOVE ADDRESS.**

1. REPORT DATE *(DD-MM-YYYY)*	2. REPORT TYPE	3. DATES COVERED *(From - To)*
June 2019	Final	

4. TITLE AND SUBTITLE

Rapid Airfield Damage Recovery Technology Integration Experiment

5a. CONTRACT NUMBER

5b. GRANT NUMBER

5c. PROGRAM ELEMENT NUMBER

6. AUTHOR(S)

Haley P. Bell, Benjamin C. Cox, Lulu Edwards, Lyan I. Garcia, Nolan R. Hoffman, Mariely Mejías-Santiago, and Jared L. Johnson

5d. PROJECT NUMBER
463347

5e. TASK NUMBER

5f. WORK UNIT NUMBER

7. PERFORMING ORGANIZATION NAME(S) AND ADDRESS(ES)

Geotechnical and Structures Laboratory & Environmental Laboratory
U.S. Army Engineer Research and Development Center
3909 Halls Ferry Road
Vicksburg, MS 39180-6199

8. PERFORMING ORGANIZATION REPORT NUMBER

ERDC TR-19-8

9. SPONSORING / MONITORING AGENCY NAME(S) AND ADDRESS(ES)

Headquarters, U.S. Air Force Civil Engineer Center
Tyndall Air Force Base, FL 32403-5319

10. SPONSOR/MONITOR'S ACRONYM(S)

AFCEC

11. SPONSOR/MONITOR'S REPORT NUMBER(S)

12. DISTRIBUTION / AVAILABILITY STATEMENT

Approved for public release; distribution is unlimited.

13. SUPPLEMENTARY NOTES

14. ABSTRACT

The traditional crater repair equipment and materials developed under the Rapid Airfield Damage Repair (RADR) program, while highly capable, are large, expensive, and logistically challenging. Research projects from 2016 and 2017 identified lighter and leaner crater repair equipment and backfill materials in an attempt to decrease some of the economic and logistical burdens on the U.S. Air Force. The RADR Technology Integration Experiment assessed the lighter and leaner equipment, materials, and methods for small crater repairs in a relative full-scale environment. The experiment was conducted in August 2017 at the Silver Flag Exercise Site located at Tyndall Air Force Base, FL. The lighter and leaner technologies were compared with the traditional crater repair process. Flowable fill, polyurethane foam, cement-stabilized soil, and geocells with granular fill were proven to be viable backfill options for repairing craters when capped with rapid-setting concrete. This effort resulted in successful crater repair solutions using the lighter and leaner technologies with limited increases in repair time. An optimized small crater repair package was developed based on the results of this experiment.

15. SUBJECT TERMS

airfield damage repair
repair airfield damage recovery
concrete
rapid-setting concrete
geotextiles
foam
flowable fill
cement-stabilized

16. SECURITY CLASSIFICATION OF:			17. LIMITATION OF ABSTRACT	18. NUMBER OF PAGES	19a. NAME OF RESPONSIBLE PERSON
a. REPORT	b. ABSTRACT	c. THIS PAGE			19b. TELEPHONE NUMBER *(include area code)*
Unclassified	Unclassified	Unclassified		118	